Quantum phase transitions in many-dipole light-matter systems

Daniele Lamberto [1,*] Omar Di Stefano [1] Stephen Hughes [2] Franco Nori [3,4,5] and Salvatore Savasta [1]

[1]Dipartimento di Scienze Matematiche e Informatiche, Scienze Fisiche e Scienze della Terra, Università di Messina, I-98166 Messina, Italy
[2]Department of Physics, Engineering Physics and Astronomy, Queen's University, Kingston, Ontario, Canada K7L 3N6
[3]Theoretical Quantum Physics Laboratory, Cluster for Pioneering Research, RIKEN, Wakoshi, Saitama 351-0198, Japan
[4]Quantum Information Physics Theory Research Team, Center for Quantum Computing, RIKEN, Wakoshi, Saitama 351-0198, Japan
[5]Physics Department, The University of Michigan, Ann Arbor, Michigan 48109, USA

(Received 23 May 2024; accepted 11 December 2024; published 14 March 2025)

A potential phase transition between a normal ground state and a photon-condensed ground state in many-dipole light-matter systems is a topic of considerable controversy, exacerbated by conflicting no-go and counter no-go theorems and often ill-defined models. We contribute to the clarification of this long-lasting debate by analyzing two specific arrangements of atoms, including a three-dimensional cubic lattice and a cavity-embedded square lattice layer—which provides a physical model for single-mode cavity QED with coupled dipoles in the thermodynamic limit. These models are shown to significantly differ from the standard Dicke model and, in the thermodynamic limit, give rise to renormalized Hopfield models. We show that a ferroelectric phase transition can, in principle, still occur and the description of the abnormal phase beyond the critical point requires the inclusion of nonlinear terms in the Holstein-Primakoff mapping. We also demonstrate how our model agrees with recent experiments.

DOI: 10.1103/PhysRevResearch.7.013271

I. INTRODUCTION

The possibility of a phase transition between a normal state and a photon condensate state within light-matter systems under the influence of electric dipolar interactions, commonly referred to as superradiant phase transition (SPT), has been a long-standing debate for many decades [1–12]. The superradiant phase is characterized by a macroscopically large number of coherent photons in the ground state. Even in recent years, several seemingly contradictory no-go and counter no-go theorems still dispute the occurrence of a SPT in such systems [13–18]. Notably, such debates are limited to the case of electric dipolar interactions, as there is a general consensus regarding the potential occurrence of a SPT in the presence of magnetic interactions, given that in these systems the so-called $\mathbf{A}^2$ term in the Coulomb gauge Hamiltonian (or $\mathbf{P}^2$ term in the multipolar gauge Hamiltonian), which prevents the SPT, can be significantly smaller or possibly absent [19,20]. However, these quadratic terms are not only required to ensure gauge invariance, but they are necessary to properly recover fundamental classical limits [21–23]. Very recently, a Dicke-like SPT has been observed in a magnetic system [24].

Recent no-go theorems demonstrated that gauge invariance forbids any phase transition to a photon condensate state when the cavity-photon mode is assumed to be spatially uniform in the region where the dipoles are located [14,16], or when magnetic interactions can be neglected [18]. However, a number of papers still support the plausibility of a SPT in many-dipole cavity-QED systems, grounded on the assumption that the system's Hamiltonian can be mapped onto a Dicke-like model [13,25,26].

This apparent SPT possibility originates from the interplay of direct electrostatic interactions and a transverse matter field term, resulting in potential compensation within the multipolar gauge. There is instances where this compensation has been effectively utilized, and outcomes have been derived [27,28]. In contrast, Ref. [8] predicts that longitudinal dipole-dipole interactions do not enable any quantum phase transition (QPT), at least for the infinite, homogeneous, and isotropic system of nonoverlapping dipoles. Moreover, there is no general agreement on the nature of this controversial QPT. According to Ref. [13], the phase transition occurring in Dicke-like models corresponds to a spontaneous polarization of the two-level systems, which does not however lead to a spontaneous transverse electric field, i.e., the QPT is ferroelectriclike. However, Ref. [29] argues that a mean field occupation in a mode of the transverse displacement field, far from the dipoles, implies a mean field in the transverse electric field. In contrast, Refs. [26,30] suggest that the nature of the QPT is gauge dependent and purely ferroelectric only in the Coulomb gauge.

To help solve these long-standing controversies, we investigate the interaction between the electromagnetic field and ordered lattices of atoms. Specifically, we consider isotropic, localized two-level atomic dipoles with threefold orientation degeneracy. When applying the two-level approximation, a consistent model of the atom requires one to consider the orientation degeneracy in one of the two levels (e.g., the excited state), since the electric dipole transition is allowed

*Contact author: daniele.lamberto@studenti.unime.it

Published by the American Physical Society under the terms of the Creative Commons Attribution 4.0 International license. Further distribution of this work must maintain attribution to the author(s) and the published article's title, journal citation, and DOI.

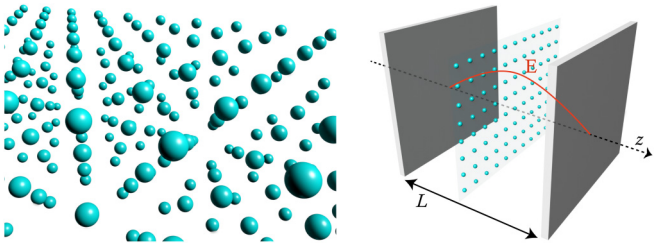

FIG. 1. Schematic of atoms arranged in a three-dimensional lattice (left) and in a cavity-embedded planar lattice (right). In the latter case, we consider radiation modes orthogonal to the atomic layer (xy plane).

only between states with different parities (e.g., between s and p orbitals). Considering these lattices, we take into account (in a simple and rigorous way) the discrete and nonoverlapping system topology, which is often overlooked during the different approximations and limits employed to derive the Dicke model. We start by considering a cubic lattice array (an isotropic system in the long-wavelength limit) and successively a cavity-embedded planar layer with a square lattice (see Fig. 1). Such arrays of dipoles, when carrying out the thermodynamic limit (number of dipoles $N \to \infty$), are well described by a light-matter Hamiltonian, having a Hopfield-like structure [31] with an additional dipole-dipole interaction term, which, as observed in a number of papers, cannot be overlooked (see, e.g., Refs. [13,26,29]). Hence, this approach provides a physically motivated model for single-mode cavity QED in the dipole approximation and in the thermodynamic limit.

II. THREE-DIMENSIONAL LATTICE

We consider a three-dimensional (3D) lattice of atoms interacting with an electromagnetic field. The radiation field is quantized by the introduction of radiation bosonic operators $a_{\mathbf{k},\lambda}$ for each mode $\mathbf{k}$ and polarization $\hat{\mathbf{e}}_\lambda$. We denote the field frequency with $\omega_k = v|\mathbf{k}|$, where $v = c/\sqrt{\epsilon_m}$ is the speed of light and ϵ_m is the dielectric constant of the surrounding medium. Hence, the vector potential of the electromagnetic field can be decomposed into plane waves as

$$\mathbf{A}(\mathbf{r}) = \sum_{\lambda} \sum_{\mathbf{k}} \mathcal{E}_k e^{i\mathbf{k}\cdot\mathbf{r}} a_{\mathbf{k},\lambda} \hat{\mathbf{e}}_\lambda + \text{H.c.}, \tag{1}$$

where $\mathcal{E}_k = \sqrt{\hbar/2\epsilon_0\epsilon_m V\omega_k}$, with V being the quantization volume, and $\hat{\mathbf{e}}_\lambda$ ($\lambda = 1, 2$) the two polarization unit vectors orthogonal to $\hat{\mathbf{k}}$. Therefore, as usual, the Hamiltonian of the free electromagnetic field is given by

$$H_{\text{ph}} = \hbar \sum_{\lambda,\mathbf{k}} \omega_k a^\dagger_{\mathbf{k},\lambda} a_{\mathbf{k},\lambda}. \tag{2}$$

In contrast, the atoms are modeled as localized charges in the sites $\mathbf{R}_n$ of a lattice. In the long-wavelength approximation, the total polarization density is thus expressed as $\mathbf{P}(\mathbf{r}) = \sum_n \mathbf{d}_n \delta(\mathbf{r} - \mathbf{R}_n)$, where $\mathbf{d}_n$ is the total electric dipole of the n^{th} atom, thus assuming nonoverlapping dipoles for different atoms. The usual electrostatic dipole-dipole interaction is given by

$$H_{\text{dip}} = \frac{1}{8\pi\epsilon_0\epsilon_m} \sum_{n\neq m} \frac{\mathbf{d}_n \cdot \mathbf{d}_m - 3(\mathbf{d}_n \cdot \hat{\mathbf{r}}_{nm})(\mathbf{d}_m \cdot \hat{\mathbf{r}}_{nm})}{r^3_{nm}}, \tag{3}$$

where $\mathbf{r}_{nm} = \mathbf{R}_n - \mathbf{R}_m$ and $\hat{\mathbf{r}}_{nm} = \mathbf{r}_{nm}/r_{nm}$ is the associated unit vector. The bare Hamiltonian of N noninteracting identical atoms is

$$H_{\text{A}} = \sum_n \frac{\mathbf{p}^2_n}{2m} + V_{\text{C}}(\mathbf{r}_n), \tag{4}$$

where $V_{\text{C}}(\mathbf{r_n})$ is the intra-atomic Coulomb potential of the n^{th} atom. For the sake of simplicity, we consider single-electron atoms. Generalization to many-electron atoms does not affect the obtained results. We then perform the two-level approximation (to derive Dicke-like models), reducing the atomic states to just the ground and excited levels, where we consider the excited states to have a threefold orientation degeneracy (see Appendix A). The bare Hamiltonian (4), in the two-level approximation, is written as

$$H_{\text{A}} = \hbar \sum_n \frac{\omega_0}{2} \sigma^z_n. \tag{5}$$

Next, we bosonify the system in the thermodynamic limit (i.e., finite density as N, $V \to \infty$) through the use of generalized Holstein-Primakoff (HP) transformations [32,33] (see Appendix B). The ensuing Hamiltonian for the matter system (according to the usual definition in condensed matter physics) is constituted by the array of dipoles with their electrostatic interactions:

$$H_{\text{mat}} = \hbar\omega_0 \sum_{\alpha,\mathbf{k}} b^\dagger_{\mathbf{k},\alpha} b_{\mathbf{k},\alpha} + \hbar \sum_{\alpha,\beta,\mathbf{k}} \chi^2 \omega_0 f_{\mathbf{k},\alpha,\beta} \times [(b_{\mathbf{k},\alpha} + b^\dagger_{-\mathbf{k},\alpha})(b_{-\mathbf{k},\beta} + b^\dagger_{\mathbf{k},\beta})], \tag{6}$$

where the first term is the thermodynamic limit of Eq. (5), the second one is the electrostatic dipole-dipole interaction in Eq. (3), $f_{\mathbf{k},\alpha,\beta} \approx [3(\hat{\mathbf{k}} \cdot \hat{\mathbf{e}}_\alpha)(\hat{\mathbf{k}} \cdot \hat{\mathbf{e}}_\beta) - \delta_{\alpha\beta}]/3$ for a simple cubic lattice in the long-wavelength limit, and $\chi = \sqrt{d^2 N/2\hbar\epsilon_0\epsilon_m V\omega_0}$ [34] (see Appendix C).

We can diagonalize the matter Hamiltonian through a Bogoliubov transformation [31,35], which leads to $H_{\text{mat}} = \hbar \sum_{\alpha,\mathbf{k}} \tilde{\omega}_{\mathbf{k},\alpha} c^\dagger_{\mathbf{k},\alpha} c_{\mathbf{k},\alpha}$, with renormalized matter frequency $\tilde{\omega}_{\mathbf{k},\alpha} = \omega_0\sqrt{1 + 4\chi^2 f_{\mathbf{k},\alpha,\alpha}}$ and bosonic eigenoperators $c_{\mathbf{k},\alpha}$. The new transverse eigenmodes describe the collective matter excitations which effectively couple with the radiation field, giving rise to a Hopfield-like model. As we will see shortly, *only in the 3D case*, the relation $\eta = \chi$ holds, where η is the normalized light-matter coupling strength.

When the matter system interacts with the radiation field solely through its polarization and neglecting the magnetic interactions, the full light-matter Hamiltonian can be obtained by applying the minimal coupling replacement in the Coulomb gauge, or equivalently in the multipolar gauge, by applying a suitable unitary transformation U to the photonic Hamiltonian Eq. (2), where U is defined as [21]

$$U = \exp\left(\frac{i}{\hbar} \int \mathbf{A}(\mathbf{r}) \cdot \mathbf{P}(\mathbf{r}) d^3\mathbf{r}\right). \tag{7}$$

This procedure leads to a Hopfield-like Hamiltonian in the multipolar gauge, which is given by (see Appendix D)

$$H = H_{\rm ph} + H_{\rm mat} + H_{\rm I_1} + H_{\rm I_2}, \tag{8}$$

with the light-matter interaction terms

$$H_{\rm I_1} = i\hbar \sum_{\alpha,\lambda,\mathbf{k}} \eta' \sqrt{\omega_k \tilde{\omega}_{\mathbf{k}}^{\perp}} (a^{\dagger}_{-\mathbf{k},\lambda} - a_{\mathbf{k},\lambda})(c^{\dagger}_{\mathbf{k},\alpha} + c_{-\mathbf{k},\alpha}) e_{\lambda_\alpha},$$

$$H_{\rm I_2} = \hbar \sum_{\alpha,\beta,\lambda,\mathbf{k}} \eta'^2 \tilde{\omega}_{\mathbf{k}}^{\perp} (c^{\dagger}_{\mathbf{k},\alpha} + c_{-\mathbf{k},\alpha})(c^{\dagger}_{-\mathbf{k},\beta} + c_{\mathbf{k},\beta}) e_{\lambda_\alpha} e_{\lambda_\beta}, \tag{9}$$

where $\tilde{\omega}_{\mathbf{k}}^{\perp} = \omega_0 \sqrt{1 + 4\eta^2 f_{\mathbf{k}}^{\perp}}$ and $\eta' = \eta\, \omega_0/\tilde{\omega}_{\mathbf{k}}^{\perp}$ are the transverse resonance frequency and light-matter coupling strength, both renormalized by the dipole-dipole interaction, respectively. The bare light-matter coupling strength η is defined by $\eta = \mathcal{E}_k \sqrt{d^2 N \omega_k/\hbar^2 \omega_0} = \sqrt{d^2 N/2\hbar\epsilon_0\epsilon_m V \omega_0}$, which, as already pointed out, coincides with χ in the 3D arrangement. The parameters $f_{\mathbf{k}}^{\perp}$ and $f_{\mathbf{k}}^{\parallel}$ represent the transverse and the longitudinal part of $f_{\mathbf{k},\alpha,\alpha}$, respectively (notice that $f_{\mathbf{k}}^{\perp} < 0$). Lastly, we defined $e_{\lambda_\alpha} = \hat{\mathbf{e}}_\lambda \cdot \hat{\mathbf{e}}_\alpha$, where the $\{\hat{\mathbf{e}}_\alpha\}$ are a generic set of orthonormal vectors chosen as a basis for the electric dipole orientation.

The dispersion relations for the transverse modes can be obtained by diagonalizing the Hopfield-like Hamiltonian (8), resulting in (see Appendix E)

$$\frac{\omega_{\mathbf{k}}^2}{\Omega_{\perp}^2} = 1 + \frac{4\eta'^2 \tilde{\omega}_{\mathbf{k}}^{\perp^2}}{\tilde{\omega}_{\mathbf{k}}^{\perp^2} - \Omega_{\perp}^2}, \tag{10}$$

where $\hbar\Omega_\perp$ is the energy of the transverse polaritons. The longitudinal modes, appearing in Eq. (8) through the term $H_{\rm mat}$, are not influenced by the interaction with photons; therefore, $\Omega_\parallel = \tilde{\omega}_{\mathbf{k}}^{\parallel}$. We observe that the same dispersion relations are obtained by diagonalizing the full light-matter Hamiltonian, without performing the initial Bogoliubov transformation on the matter subsystem, as explicitly shown in Appendix E. Moreover, the same results are obtained in the Coulomb gauge, if gauge invariance is treated with a suitable approach [21,36–38], as further elaborated on in Appendix E, thereby highlighting the consistency of our results. Notice that the dispersion relation in Eq. (10), obtained by diagonalizing the Hopfield model, also agrees with the results obtained solving the corresponding Maxwell equations in a semiclassical approach.

Let us now discuss the possibility for the system to undergo a QPT. Equation (10) is formally derived by the diagonalization of a Hopfield-like model with effective coupling constant η' [Eq. (8)]. Such a model, as is well known, does not exhibit any radiation induced QPT [Fig. 2(a)] [40] for a finite value of η'. However, the dipole-dipole interactions in Hamiltonian (6) enable the occurrence of a QPT transition, as testified by the softening of the transverse renormalized matter frequency $\tilde{\omega}_{\mathbf{k}}^{\perp}$ at increasing dipole-dipole interaction strengths η [Fig. 2(b)]. This ferroelectric QPT occurs even without including retardation effects and gives rise to a transverse polarization condensate $\langle P_{\mathbf{k}}^{\perp}\rangle \neq 0$, as explicitly shown in Appendix G. In particular, for isotropic systems in the long-wavelength approximation, the QPT can be achieved for $\eta > \eta_c \approx \sqrt{3}/2$. In contrast, near a QPT, $\eta' = \eta\, \omega_0/\tilde{\omega}_{\mathbf{k}}^{\perp}$ is not a suitable parameter given that it diverges for $\eta \to \eta_c$. This relation between η and η' explains why the Hopfield model remains a valid description even for many-dipole systems approaching a ferroelectric QPT.

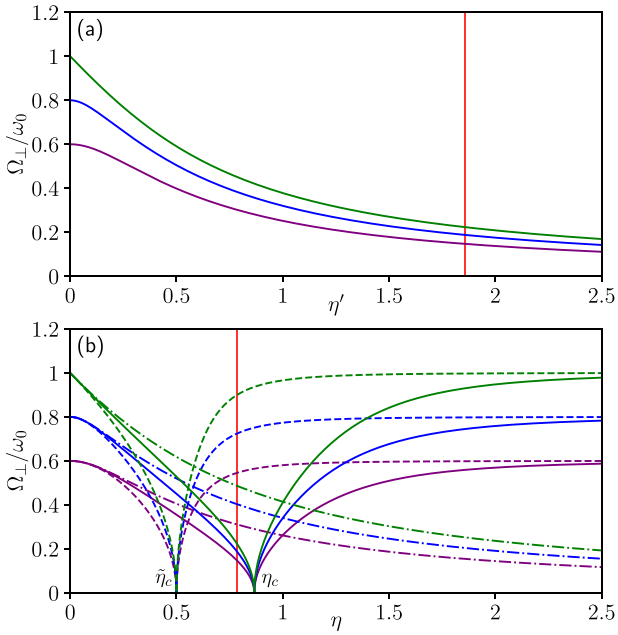

FIG. 2. Lower polariton frequencies for different modes $\omega_k/\omega_0 = 0.6$ (purple), 0.8 (blue), and 1 (green). The vertical red line indicates the coupling strength $\eta' = 1.83$ measured in Ref. [39], corresponding to $\eta = 0.78$. (a) Lower polaritons as functions of η'. (b) Comparison of lower polaritons obtained from the renormalized Hopfield-like model (solid lines), Dicke-like model (dashed lines), and Hopfield model without dipole-dipole interactions (dash-dotted lines) vs η.

It is noteworthy that neither the critical point nor the ground-state transverse polarization in the condensed phase is influenced by the interaction with the photon field. Instead, the latter is determined solely by the strength of dipolar interactions, as anticipated for a ferroelectric phase transition. However, this QPT involves transverse matter excitations and, consequently, affects also transverse polaritons. We can calculate the transverse dispersions in the condensed phase using higher-order terms in the HP mapping and, through a minimization procedure, we obtain (see Appendix G)

$$\frac{\omega_{\mathbf{k}}^2}{\Omega_{\perp}^2} = 1 + \frac{\omega_0^2/f_{\mathbf{k}}^{\perp}}{\omega_0^2\left(1 - 16\eta^4 f_{\mathbf{k}}^{\perp^2}\right) + \Omega_{\perp}^2}, \quad \text{for } \eta > \eta_c, \tag{11}$$

while Eq. (10) is valid only for $\eta < \eta_c$. In particular, the ferroelectric condensation of the dipoles system occurring for $\eta > \eta_c$ determines a macroscopic transverse polarization density $\langle P_{\mathbf{k}}^{\perp}\rangle$, which, although not affected by the interaction with the photon field, induces a macroscopic occupation of $\langle D_{\mathbf{k}}\rangle \neq 0$. The latter, *in the multipolar gauge*, is proportional to the field momentum, i.e., $\langle a_{\mathbf{k},\lambda}\rangle \neq 0$. This occurrence induced recent works [26,30] to characterize the phase transition as ferroelectric or superradiant depending on the gauge choice. In contrast, we obtain $\langle D_{\mathbf{k}}\rangle = \langle P_{\mathbf{k}}^{\perp}\rangle$, which, from the definition of the displacement field, implies $\langle E_{\mathbf{k}}^{\perp}\rangle = 0$ (see Appendix G). We observe that quantities such as $D_{\mathbf{k}}$ and the transverse electric field $E_{\mathbf{k}}^{\perp}$ are physical quantities, the expectation values

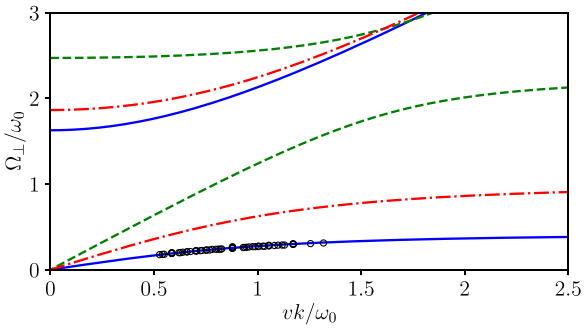

FIG. 3. Comparison of transverse dispersion curves obtained for the renormalized Hopfield-like model [Eq. (10)] (blue solid), Dicke-like model (green dashed), and Hopfield model without dipolar interactions (red dash-dotted) (coupling constant $\eta' = 1.83$). Experimental data (black dots) from Ref. [39] are included, which use arrays of coupled metal nanoparticles, showing a strong agreement with the proposed model.

of which are *not* gauge dependent. However, operators such as the field momentum and the photon creation and destruction operators are nonphysical quantities which can be used only as calculation tools [41], and thus are not suitable to characterize physical processes.

We now briefly discuss a potential cancellation procedure which can possibly justify the usual Dicke model [13,26,30,42]. Such a procedure is based on the interplay between electrostatic terms in Eq. (6) (the dipole-dipole interaction) and the interatomic part of H_{I_2} (which originates from light-matter interaction). In particular, a key step of this procedure is the decomposition of the polarization field $\mathbf{P}(\mathbf{r})$ in its intra- and interatomic, longitudinal and transverse parts. After the compensation between these two terms, to obtain the Dicke model, a single-polarization single-mode approximation for the radiation and a strict two-level approximation for the dipoles are employed. The remaining intra-atomic part of H_{I_2}, in the strict two-level approximation, becomes proportional to the identity operator. However, this term results from the combination of electrostatic and transverse contributions and cannot be neglected when the orientation degree of freedom of the dipoles is considered. Following this procedure, the Dicke-like multipolar-gauge Hamiltonian for a single mode is obtained (e.g., see Ref. [26]):

$$\tilde{H} = \hbar\omega_0 b^\dagger b + \hbar\omega_k a^\dagger a - i\hbar\eta\sqrt{\omega_k\omega_0}(a^\dagger - a)(b^\dagger + b). \qquad (12)$$

This model, in contrast with the previous Hopfield-like one in Eq. (8), predicts a light-induced QPT (superradiant QPT, or SPT), for a critical value of the coupling $\tilde{\eta}_c = 0.5$ [26,32].

Figure 2(b) shows the lower polariton resonances derived from the Hamiltonians in Eq. (8) (solid lines) and Eq. (12) (dashed lines). The different modes displayed all exhibit a softening, indicative of a quantum phase transition, all vanishing at the respective critical coupling values, η_c and $\tilde{\eta}_c$. For completeness, we also plot the polariton modes computed using a pure Hopfield model, where dipolar interactions are neglected. Unlike the previous cases, the resulting lower polaritons do not exhibit any indication of a QPT.

In Fig. 3, we compare the dispersion curves for the transverse and longitudinal sectors in both Hopfield-like [Eq. (8)] and Dicke-like [Eq. (12)] models. In particular, Fig. 3 shows the theoretical predictions of both models and the experimental data taken from Ref. [39] (using arrays of coupled metal nanoparticles). The data set reports measurements of the lower polariton branch of a three-dimensional artificial crystal made of spatially separated gold nanoparticles [43] (see also Appendix H). The explicit fit parameters are provided in the corresponding Ref. [39]. The nanoparticles, each supporting triply degenerate localized dipolar surface plasmons, couple through dipole-dipole interactions, giving rise to collective plasmons that extend over the whole metamaterial. These excitations can be described in terms of collective bosonic operators, analogously to the atomic collective excitations (in the thermodynamic limit) that we considered above. These artificial gold crystals can reach very high light-matter interaction strengths. Hence, they represent an ideal testbed for discerning among the different models considered, and help solve the long-standing debate about QPTs in many-dipoles systems.

The measurements in Fig. 3 have already been compared in Ref. [39], but with a Hopfield model where the light-matter coupling strength was renormalized with respect to transverse matter polaritonic frequency, which corresponds to our η', showing excellent agreement. However, probably for this reason, in Ref. [39] it was not pointed out that a QPT could occur for higher couplings (Fig. 3). Here, we make clear the relationship between the bare and renormalized parameters involved in the modeling. The high coupling achieved in the experiment ($\eta' = 1.83$, corresponding to $\eta = 0.78 > \tilde{\eta}_c$), according to the Dicke-like model, would imply a condensed phase and a dispersion relation, shown in Fig. 3, strongly differing from the data. However, we point out that, beyond the critical point, the dispersion relation for the atomic system and for the artificial crystal may present quantitative differences owing to the different nonlinear response of these systems. Furthermore, we notice that the achieved coupling strength $\eta = 0.78$ (red vertical line in Fig. 2) is not far from $\eta_c \approx 0.87$, and the consequent softening of $\tilde{\omega}^\perp_{\mathbf{k}}$, which dictates the asymptotic behavior of the lower polariton, can be appreciated. We also observe that the Hopfield model without dipole-dipole interactions fails to reproduce correctly the data.

III. TWO-DIMENSIONAL LATTICE

In this section, we consider a system composed of a two-dimensional (2D) layer of atoms, identified as the xy plane, interacting with a radiation field confined in an ideal cavity [e.g., with dielectric mirrors; see Fig. 1(b)]. Such a system is of particular interest since it represents a realizable configuration for single-mode cavity QED in the dipole approximation and in the thermodynamic limit, useful for testing the validity of the models for many-dipole systems.

This planar configuration naturally induces a decomposition of the vector potential in terms of $\mathbf{k}_\parallel$, the in-plane discrete component of the wave vector with corresponding quantization surface S, and its orthogonal component k_z, quantized by the length of the cavity L, as

$$A(\mathbf{r}) = \sum_{\lambda,\mathbf{k}_\parallel}\sum_{k_z>0} \mathcal{E}_k e^{i\mathbf{k}_\parallel\cdot\mathbf{r}_\parallel}\hat{\mathbf{e}}_\lambda \times \left(e^{ik_z z}a_{l,\mathbf{k}_\parallel,k_z,\lambda} + e^{-ik_z z}a_{r,\mathbf{k}_\parallel,k_z,\lambda}\right) + \text{H.c.}, \qquad (13)$$

where $\mathcal{E}_k = \sqrt{\hbar/2\epsilon_0\epsilon_m\omega_k SL}$ and $\omega_k = v\sqrt{\mathbf{k}_\parallel{}^2 + k_z^2}$. In this expression, we introduced the left and right creation operators $a_{l(r),\mathbf{k}_\parallel,k_z,\lambda} \equiv a_{\mathbf{k}_\parallel,\pm k_z,\lambda}$, where the index l (r) is associated with the $+(-)$ sign. If we consider only modes orthogonal to the planar surface, $\mathbf{k}_\parallel = \mathbf{0}$ and thus $\mathbf{k} = k_z\hat{\mathbf{z}}$, Eq. (13) considerably simplifies given that the two polarization vectors $\hat{\mathbf{e}}_\lambda$ now lie in the xy plane and the bosonic operators become independent on $\mathbf{k}_\parallel$, i.e., $a_{l(r),\mathbf{k}_\parallel=\mathbf{0},k_z,\lambda} \equiv a_{l(r),k_z,\lambda}$. Defining the even and odd radiation modes operators as $a_{e(o),k_z,\lambda} = (a_{l,k_z,\lambda} \pm a_{r,k_z,\lambda})/\sqrt{2}$, the Hamiltonian of the free electromagnetic field can be written as [44]

$$H_{\rm ph} = \hbar \sum_\lambda \sum_{j=e,o} \sum_{k_z>0} \omega_{k_z} a^\dagger_{j,k_z,\lambda} a_{j,k_z,\lambda}. \tag{14}$$

Following a procedure analogous to that previously applied to the 3D dipoles lattice, we first perform the two-level approximation taking into account the dipole orientations, and successively construct 2D collective bosonic operators $b_{\mathbf{k}_\parallel}$. For incidence orthogonal to the planar surface ($\mathbf{k}_\parallel = 0$), the matter Hamiltonian reads

$$H_{\rm mat} = \hbar\omega_0 \sum_\alpha b^\dagger_\alpha b_\alpha + \hbar \sum_{\alpha,\beta} \chi^2 \omega_0 f_{\mathbf{z},\alpha,\beta}(b_\alpha + b^\dagger_\alpha)(b_\beta + b^\dagger_\beta), \tag{15}$$

where $b_\alpha \equiv b_{\mathbf{k}_\parallel=0,\alpha}$ and the structure-dependent factor for the 2D square lattice is $\chi = \sqrt{d^2\mu/\hbar\epsilon_0\epsilon_m a^3\omega_0}$, with a being the lattice constant and $\mu \approx 6.78/4\pi$ (see Appendix C).

As in the 3D lattice case, the Hamiltonian in Eq. (15) can be diagonalized through the introduction of eigenoperators c_α, with a corresponding renormalized frequency $\tilde{\omega}_\alpha = \omega_0\sqrt{1 + 4\chi^2 f_{\mathbf{z},\alpha,\alpha}}$. Therefore, the light-matter Hamiltonian in the multipolar gauge reads

$$H = H_{\rm ph} + H_{\rm mat} + H_{\rm I_1} + H_{\rm I_2}, \tag{16}$$

with the light-matter interaction terms

$$H_{\rm I_1} = i\hbar \sum_{\lambda,k_z>0} \eta' \sqrt{\omega_{k_z}\tilde{\omega}^\perp}\left(a^\dagger_{e,k_z,\lambda} - a_{e,k_z,\lambda}\right)\left(c^\dagger_\lambda + c_\lambda\right),$$
$$H_{\rm I_2} = \hbar \sum_{\lambda,k_z>0} \eta'^2 \tilde{\omega}^\perp (c^\dagger_\lambda + c_\lambda)(c^\dagger_\lambda + c_\lambda), \tag{17}$$

where $\eta' = \eta\,\omega_0/\tilde{\omega}^\perp$ is the renormalized light-matter coupling for the planar layer, with $\eta = \sqrt{d^2 N/\hbar\epsilon_0\epsilon_m SL\omega_0}$ and $\tilde{\omega}^\perp$ the renormalized transverse matter frequency. We have chosen the same basis for the dipole orientation and the radiation polarization. When considering a single k_z and a single transverse polarization mode, the Hamiltonian (16) reduces to that of a two coupled harmonic oscillators model, as the Dicke Hamiltonian in the thermodynamic limit, but with the presence of the so-called self-polarization term, $\mathbf{P}^2$ ($H_{\rm I_2}$).

From the total Hamiltonian (16), we can derive the transverse dispersion relation (see Appendix E):

$$\frac{\Omega_\perp^2 - \tilde{\omega}^{\perp 2}}{2\tilde{\omega}^\perp} + 2\eta'^2\tilde{\omega}^\perp \sum_{k_z>0} \frac{\Omega_\perp^2}{\omega_{k_z}^2 - \Omega_\perp^2} = 0. \tag{18}$$

In the single-mode approximation, such a relation reduces to the dispersion relation derived from a renormalized Hopfield-like model, as in the 3D lattice. This is to be expected due to the formal equivalence between the structures of Hamiltonians (8) and (16). In both cases, we observe that the dipole-dipole structure factor χ depends on a^{-3}. However, the 2D and 3D lattices exhibit different scaling behaviors of the light-matter coupling with respect to the lattice constant, as further discussed in Appendix C. In the 3D lattice, η can be directly related to the volumetric density ρ, yielding the proportionality $\eta^2 \propto \rho \propto a^{-3}$. In contrast, for the 2D lattice, this proportionality does not hold because the charges are arranged in a planar structure with a surface density $\sigma \propto a^{-2}$, which appears in the light-matter coupling η together with the cavity length L. Consequently, η cannot be straightforwardly connected to χ, which, notably, is the key factor driving the QPT. Moreover, we emphasize that in this case the cancellation procedure loses meaning given that the couplings governing the dipole-dipole and the light-matter interactions, χ and η respectively, are different, despite both being dependent on the atomic dipole moment. These evidences further confirm the ferroelectric nature of the QPT.

IV. DISCUSSION AND CONCLUSIONS

We have shown that the standard Dicke model, a widespread description of many-dipole cavity-QED systems (in the dipole and single-mode approximations), is not a suitable description for simple systems of two-level atomic dipoles with the usual orientation degeneracy, even when dipole-dipole interactions are considered. In contrast, the Hopfield model offers a more accurate representation for systems of nonoverlapping dipolar quantum emitters, with its parameters renormalized to account for electrostatic dipole-dipole interactions. Our analysis agrees with recent experimental results on artificial crystals made of gold nanoparticles, which display analogous linear optical properties. Although the Hopfield model does not admit any radiation-induced QPT, the system of dipolar quantum emitters can still undergo, at least in principle, a QPT when the dipole-dipole interaction strength reaches the critical value $\chi_c = \sqrt{3}/2$ (for a 3D lattice of atoms), different from the value predicted by the corresponding Dicke-like model. The potential QPT induces a macroscopic transverse matter polarization field in the system ground state which, in turn, affects the interaction between the matter system and light, thereby modifying the dispersion relations for transverse polaritons in the ferroelectric phase.

Our results clarify the ferroelectric nature of the predicted QPT, given the following:

(i) The QPT occurs even without including the transverse interaction of the matter field with photons, and its inclusion does not modify either the critical point or the transverse polarization condensate.

(ii) The critical parameter χ does not correspond to the light-matter coupling strength (although both depend on d^2) and, in contrast to the latter, χ does not depend on the cavity length (in the 2D case).

(iii) The ground state does not display any coherent macroscopic transverse electric or magnetic fields.

However, we stress that this QPT is challenging to realize experimentally, as achieving the required high coupling

strength [45] necessitates densities approaching the point of system solidification, as already noticed in previous works [46,47]. Owing to the small size of the fine structure constant, $\chi \approx 10^{-3}\, r^2\lambda_0/a^3$ is usually far from the critical value χ_c, with $\lambda_0 = 2\pi v/\omega_0$ being the matter wavelength and r the mean atomic radius. Notice, also, that $4r < a$ is typically required to reasonably avoid overlap of the emitter wave functions. It would be interesting to extend this analysis to various lattices of emitters, particularly to systems of anisotropic quantum emitters where orientation degeneracy is lifted. Furthermore, all the results presented here have been derived under the assumption of a closed quantum system. Investigating how these findings are altered by explicitly accounting for the interaction of the matter and light components with their respective thermal reservoirs could be a topic for future research [48].

ACKNOWLEDGMENTS

S.H. thanks the Natural Sciences and Engineering Research Council of Canada (NSERC), the National Research Council of Canada (NRC), the Canadian Foundation for Innovation (CFI), and Queen's University, Canada, for funding support. F.N. is supported in part by: Nippon Telegraph and Telephone Corporation (NTT) Research, the Japan Science and Technology Agency (JST) [via the CREST Quantum Frontiers program Grant No. JPMJCR24I2, the Quantum Leap Flagship Program (Q-LEAP), and the Moonshot R&D Grant No. JPMJMS2061], and the Office of Naval Research (ONR) Global (via Grant No. N62909-23-1-2074). S.S. acknowledges support by the Army Research Office (ARO) through Grant No. W911NF1910065.

APPENDIX A: TWO-LEVEL APPROXIMATION WITH THREEFOLD DEGENERACY

In the derivation of the Hamiltonians presented in this paper, we reduce the atomic states to two levels. Here we consider isotropic atoms with inversion symmetry. Owing to isotropy and electric dipole selection rules, a consistent model requires that the excited state is threefold degenerated, while the ground state is unique (p-like and s-like orbitals). We denote with $|-\rangle_n$ the ground state of the n^{th} atom, while we use $|+_\alpha\rangle_n$ for the excited states in the three different orientations ($\alpha \in \{1, 2, 3\}$), which are orthogonal to each other. Thereby, we can define generalized orientation-dependent Pauli operators, describing the transition in the respective orientation. In particular, we define the generalized $S_n^z = \frac{\hbar}{2}\sigma_n^z$ operator (where $n = 1, \ldots, N$ is the index of the atom) such that it satisfies the usual relations for spin-$\frac{1}{2}$ systems:

$$\begin{aligned} S^z|-\rangle &= -\frac{\hbar}{2}|-\rangle, \\ S^z|+_\alpha\rangle &= \frac{\hbar}{2}|+_\alpha\rangle, \end{aligned} \qquad \forall\, \alpha \in \{1, 2, 3\}\,, \tag{A1}$$

where we dropped the atomic index n for notational convenience. Compactly, we can write the previous relations as $S^z|m_\alpha\rangle = \hbar m|m_\alpha\rangle$, where $|m_\alpha\rangle \in \{|-\rangle, |+_\alpha\rangle\}$ and $m \in \{-\frac{1}{2}, \frac{1}{2}\}$ are the respective eigenvalues.

Analogously, we define the orientation-dependent raising and lowering operators $S_\alpha^\pm = \hbar\sigma_\alpha^\pm$ which raise or lower the state in the corresponding direction, characterized by the following properties:

$$\begin{aligned} S_\alpha^+|-\rangle &= \hbar|+_\alpha\rangle, \\ S_\alpha^+|+_\beta\rangle &= 0, \\ S_\alpha^-|-\rangle &= 0, \\ S_\alpha^-|+_\beta\rangle &= \delta_{\alpha,\beta}\hbar|-\rangle. \end{aligned} \qquad \forall\, \alpha, \beta \in \{1, 2, 3\}\,. \tag{A2}$$

In the basis $\{|+_1\rangle, |+_2\rangle, |+_3\rangle, |-\rangle\}$, these Pauli operators have the following matrix representation:

$$\sigma_\alpha^- = \begin{pmatrix} 0 & 0 & 0 & 0 \\ 0 & 0 & 0 & 0 \\ 0 & 0 & 0 & 0 \\ \delta_{\alpha 1} & \delta_{\alpha 2} & \delta_{\alpha 3} & 0 \end{pmatrix}, \tag{A3}$$

$$\sigma_\alpha^+ = (\sigma_\alpha^-)^\dagger, \tag{A4}$$

$$\sigma_\alpha^x = \sigma_\alpha^- + \sigma_\alpha^+, \tag{A5}$$

$$\sigma_\alpha^y = i(\sigma_\alpha^- - \sigma_\alpha^+), \tag{A6}$$

$$\sigma^z = \begin{pmatrix} 1 & 0 & 0 & 0 \\ 0 & 1 & 0 & 0 \\ 0 & 0 & 1 & 0 \\ 0 & 0 & 0 & -1 \end{pmatrix}. \tag{A7}$$

It can be shown that these operators satisfy generalized commutation relations expected from angular-momentum-like operators, such as $[S^z, S_\alpha^\pm] = \pm\hbar S_\alpha^\pm$. Using these notions, we can express the dipole moment operator of the n^{th} atom as

$$\mathbf{d}_n = \sum_\alpha d_{n,\alpha}\mathbf{e}_\alpha = \sum_\alpha d\sigma_{n,\alpha}^x\mathbf{e}_\alpha = \sum_\alpha d(\sigma_{n,\alpha}^- + \sigma_{n,\alpha}^+)\mathbf{e}_\alpha, \tag{A8}$$

where $\mathbf{e}_\alpha$ is the unit vector in the α direction. We considered the dipole moment having the same modulus in the different directions. Notice that the definition in Eq. (A8) is consistent with the selection rules prohibiting the transition between states of the same parity.

APPENDIX B: GENERALIZED HOLSTEIN-PRIMAKOFF TRANSFORMATIONS

In this section, we define generalized Holstein-Primakoff transformations mapping the spin operators, Eqs. (A1) and (A2), into bosonic operators $b_{\mathbf{k}}$. Initially, we will bosonize a two-level system with a threefold degenerated excited state, and successively extend the mapping to a collection of such systems.

To this end, we first derive a closed form for the action of $S_\alpha^\pm$ on a generic state $|m_\beta\rangle$. We notice that, by definition, $S_\alpha^\pm|m_\beta\rangle = c_{\alpha\beta}^\pm|m \pm 1_\beta\rangle$. The coefficients $c_{\alpha\beta}^\pm$ are determined by the following relation:

$$|c_{\alpha\beta}^\pm|^2 = \|S_\alpha^\pm|m_\beta\rangle\|^2 = \langle m_\beta|S_\alpha^\mp S_\alpha^\pm|m_\beta\rangle \tag{B1}$$

$$= \hbar^2[s(s + \delta_{\alpha\beta}) - m(m \pm \delta_{\alpha\beta})], \tag{B2}$$

where in our case $s = \frac{1}{2}$. Thus, in accordance with the Condon-Shortley phase convention, we select the coefficients

to be real and positive:

$$c^{\pm}_{\alpha\beta} = \hbar\sqrt{s(s+\delta_{\alpha\beta}) - m(m\pm\delta_{\alpha\beta})} \tag{B3}$$

$$= \hbar\sqrt{(s\mp m)(s\pm m+\delta_{\alpha\beta})}. \tag{B4}$$

Introducing the operator $N = s + S^z/\hbar$, which represents the number of excitations in the system, we observe that the eigenvectors of S^z can be relabeled, as they are evidently also eigenvectors of N. Thus, we have $N|n_\alpha\rangle = n|n_\alpha\rangle$, with $n = \frac{1}{2} + m \in \{0, 1\}$. We notice that $n = 0$ if the system is in the ground state, while $n = 1$ if the system is in its excited state, consistently with the interpretation of the operator N. From Eqs. (A1), (A2), and (B4), the actions of S^z and $S^{\pm}_\alpha$ on $|n_\beta\rangle$ in terms of the excitation number are

$$S^z|n_\beta\rangle = \hbar\big(n - \tfrac{1}{2}\big)|n_\beta\rangle, \tag{B5}$$

$$S^+_\alpha|n_\beta\rangle = \hbar\sqrt{n+\delta_{\alpha\beta}}\sqrt{1-n}|n+1_\beta\rangle$$

$$= \hbar\delta_{\alpha\beta}\sqrt{n+1}\sqrt{1-n}|n+1_\beta\rangle, \tag{B6}$$

$$S^-_\alpha|n_\beta\rangle = \hbar\sqrt{1-(n-\delta_{\alpha\beta})}\sqrt{n}|n-1_\beta\rangle$$

$$= \hbar\delta_{\alpha\beta}\sqrt{1-(n-1)}\sqrt{n}|n-1_\beta\rangle, \tag{B7}$$

where in the last steps of Eqs. (B6) and (B7) we exploited the isomorphism between the two members. These relations are indeed consistent with the physical interpretation of $S^{\pm}_\alpha$, since we expect the operator $S^+_\alpha(S^-_\alpha)$ to be able to increase (decrease) the quantum number only in the α direction.

We can now define bosonic operators for the different orientations b_α, which satisfy the usual properties:

$$b_\alpha|n_\beta\rangle = \delta_{\alpha\beta}\sqrt{n}|n-1_\beta\rangle, \tag{B8}$$

$$b^\dagger_\alpha|n_\beta\rangle = \delta_{\alpha\beta}\sqrt{n+1}|n+1_\beta\rangle, \tag{B9}$$

$$b^\dagger_\alpha b_\alpha|n_\beta\rangle = \delta_{\alpha\beta}n|n_\beta\rangle, \tag{B10}$$

$$[b_\alpha, b^\dagger_\beta] = \delta_{\alpha\beta}. \tag{B11}$$

Therefore, using the previous relations (B5)–(B7), we can establish the generalized Holstein-Primakoff transformations for a single two-level system, which relate the spin to the bosonic operators, as

$$S^+_\alpha = \hbar b^\dagger_\alpha\sqrt{1-\sum_\beta b^\dagger_\beta b_\beta}, \tag{B12}$$

$$S^-_\alpha = \hbar\sqrt{1-\sum_\beta b^\dagger_\beta b_\beta}\; b_\alpha, \tag{B13}$$

$$S^z = \hbar\left(\sum_\beta b^\dagger_\beta b_\beta - \frac{1}{2}\right). \tag{B14}$$

In the limit of low excitations in the system (corresponding to a low average excitation per site), we can expand the radicals in Eqs. (B12) and (B13) and retain only the lowest power term in each expression, which yields

$$S^{-(+)}_\alpha \approx \hbar b^{(\dagger)}_\alpha. \tag{B15}$$

Finally, we consider a collection of N spin-$\frac{1}{2}$ identical systems and construct collective operators in the three-dimensional $\mathbf{k}$ space. In particular, labeling with $b_{n,\alpha}$ the bosonic operator associated with the nth site, we define the collective bosonic operators $b_{\mathbf{k},\alpha}$ as

$$b_{\mathbf{k},\alpha} = \frac{1}{\sqrt{N}}\sum_n e^{-i\mathbf{k}\cdot\mathbf{R}_n}b_{n,\alpha}. \tag{B16}$$

It can be readily verified that these operators obey the commutation relations $[b_{\mathbf{k},\alpha}, b_{\mathbf{k}',\beta}] = \delta_{\mathbf{k}\mathbf{k}'}\delta_{\alpha\beta}$. In the derivation of the Hamiltonians, we will make use of the relation $\sum_n b^\dagger_{n,\alpha}b_{n,\alpha} = \sum_{\mathbf{k}} b^\dagger_{\mathbf{k},\alpha}b_{\mathbf{k},\alpha}$, which can be easily demonstrated. Furthermore, using Eqs. (B15) and (B16), we derive the relations for the low-excitation regime:

$$\sum_{n=1}^{N} e^{-(+)i\mathbf{k}\cdot\mathbf{R}_n}S^{-(+)}_{n,\alpha} = \hbar\sqrt{N}b^{(\dagger)}_{\mathbf{k},\alpha}. \tag{B17}$$

APPENDIX C: DIPOLE-DIPOLE INTERACTIONS

The electrostatic dipole-dipole interaction between two localized charges is expressed by

$$V_{\rm dip}(\mathbf{R}_1, \mathbf{R}_2) = \frac{1}{4\pi\epsilon_0\epsilon_m}\frac{\mathbf{d}_1\cdot\mathbf{d}_2 - 3(\mathbf{d}_1\cdot\hat{\mathbf{r}}_{12})(\mathbf{d}_2\cdot\hat{\mathbf{r}}_{12})}{r^3_{12}}. \tag{C1}$$

Therefore, the dipole-dipole Hamiltonian contribution for a system of localized particles is given by

$$H_{\rm dip} = \frac{1}{2}\sum_{n\neq m} V_{dip}(\mathbf{R}_n, \mathbf{R}_m), \tag{C2}$$

which, upon the introduction of the definition Eq. (C1), coincides with Eq. (3) of the main text. We can now perform the two-level approximation (A8) and successively proceed to the bosonization of the system in the thermodynamic limit through the use of the generalized Holstein-Primakoff transformations (see Sec. B). In the following, we will investigate separately the cases of 3D and 2D lattices.

1. 3D lattice dipole-dipole interactions

For a 3D ordered lattice, in the long-wavelength approximation, we can express the matter field in terms of collective bosonic operators $b_{\mathbf{k},\alpha}$. Therefore, after the bosonization, the dipole-dipole term in Eq. (C2) is given by

$$H_{\rm dip} = \sum_{\alpha,\beta,\mathbf{k}} F_{\mathbf{k},\alpha,\beta}(b_{\mathbf{k},\alpha} + b^\dagger_{-\mathbf{k},\alpha})(b_{-\mathbf{k},\beta} + b^\dagger_{\mathbf{k},\beta}), \tag{C3}$$

where we have defined structure-dependent factor $F_{\mathbf{k},\alpha,\beta}$ as

$$F_{\mathbf{k},\alpha,\beta} = \frac{d^2}{8\pi\epsilon_0\epsilon_m}\sum_{l\neq 0}\frac{\cos\mathbf{k}\cdot\mathbf{r}_l}{r^3_l}[\delta_{\alpha,\beta} - 3(\hat{\mathbf{e}}_\alpha\cdot\hat{\mathbf{r}}_l)(\hat{\mathbf{e}}_\beta\cdot\hat{\mathbf{r}}_l)], \tag{C4}$$

and we used the translational symmetry of the system. $\mathbf{r}_l \equiv \mathbf{r}_{0l}$ is the distance of the lth site from the origin, which is the only point excluded in the summation ($l \neq 0$). Such a factor can be approximated, in the long-wavelength limit (corresponding to the neighborhood of the Γ point in the crystal), as [34]

$$\sum_{l\neq 0}\frac{\cos\mathbf{k}\cdot\mathbf{r}_l}{r^3_l}[\delta_{\alpha,\beta} - 3(\hat{\mathbf{e}}_\alpha\cdot\hat{\mathbf{r}}_l)(\hat{\mathbf{e}}_\beta\cdot\hat{\mathbf{r}}_l)]$$

$$\approx \frac{4\pi}{3v}\rho[3(\hat{\mathbf{k}}\cdot\hat{\mathbf{e}}_\alpha)(\hat{\mathbf{k}}\cdot\hat{\mathbf{e}}_\beta) - \delta_{\alpha\beta}], \tag{C5}$$

where the factor v depends on the lattice structure and it is equal to $v = 1$ for sc, $v = 2^{-1/2}$ for fcc, and $v = 4 \times 3^{-3/2}$ for bcc lattices. Thus, we can define the factor $f_{\mathbf{k},\alpha,\beta} \approx [3(\hat{\mathbf{k}} \cdot \hat{\mathbf{e}}_\alpha)(\hat{\mathbf{k}} \cdot \hat{\mathbf{e}}_\alpha) - \delta_{\alpha\beta}]/3$, which directly follows from the form of $F_{\mathbf{k},\alpha,\beta}$. Hence, we have for a three-dimensional lattice in the long-wavelength approximation,

$$F_{\mathbf{k},\alpha,\beta} = \frac{d^2\rho}{2\epsilon_0\epsilon_m}\frac{3(\hat{\mathbf{k}} \cdot \hat{\mathbf{e}}_\alpha)(\hat{\mathbf{k}} \cdot \hat{\mathbf{e}}_\beta) - \delta_{\alpha\beta}}{3} = \hbar\chi^2\omega_0 f_{\mathbf{k},\alpha,\beta} = \hbar\eta^2\omega_0 f_{\mathbf{k},\alpha,\beta}, \tag{C6}$$

where we used the relation $\chi^2\omega_0 = d^2\rho/2\hbar\epsilon_0\epsilon_m$ and the equality $\chi = \eta$, *valid only in the three-dimensional case*.

2. 2D lattice dipole-dipole interactions

We repeat the previous procedure for a square (bidimensional) lattice. The main difference from the three-dimensional case is that the system has not any discrete translational invariance along the z axis, given that the charges are ordered in a planar structure on the xy plane. Hence, the mode decomposition (and thus the matter bosonic operators $b_{\mathbf{k}_\parallel,\alpha}$) only depends on $\mathbf{k}_\parallel$. Therefore, for incidence orthogonal to the plane surface ($\mathbf{k}_\parallel = 0$), Eq. (C3) becomes

$$H_{\text{dip}} = \sum_{\alpha,\beta} F_{\alpha,\beta}(b_\alpha + b_\alpha^\dagger)(b_\beta + b_\beta^\dagger), \tag{C7}$$

where the factor $F_{\alpha,\beta}$ reduces to

$$F_{\alpha,\beta} = \frac{d^2}{8\pi\epsilon_0\epsilon_m}\sum_{l\neq 0}\frac{1}{r_l^3}[\delta_{\alpha,\beta} - 3(\hat{\mathbf{e}}_\alpha \cdot \hat{\mathbf{r}}_l)(\hat{\mathbf{e}}_\beta \cdot \hat{\mathbf{r}}_l)]. \tag{C8}$$

In particular, this expression is independent of the wave vector and, thus, it does not rely on the limit of long wavelength to be evaluated. In fact, a being the lattice constant, Eq. (C8) can be evaluated as

$$F_{\alpha,\beta} = \frac{d^2\mu}{\epsilon_0\epsilon_m a^3}\frac{3(\hat{\mathbf{z}} \cdot \hat{\mathbf{e}}_\alpha)(\hat{\mathbf{z}} \cdot \hat{\mathbf{e}}_\beta) - \delta_{\alpha\beta}}{3} = \hbar\chi^2\omega_0 f_{\mathbf{z},\alpha,\beta}, \tag{C9}$$

where we defined for the 2D lattice

$$\chi = \sqrt{\frac{d^2\mu}{\hbar\epsilon_0\epsilon_m a^3\omega_0}}, \tag{C10}$$

$$\mu = \frac{3}{4\pi}\left[\sum_{n_x>0} n_x^{-3} + \sum_{n_x,n_y>0}\left(n_x^2 + n_y^2\right)^{-3/2}\right] \approx \frac{6.78}{4\pi}. \tag{C11}$$

As pointed out in the main text, the crucial difference between the two-dimensional and three-dimensional cases is the dependence of the light-matter coupling on the lattice constant a. First, we notice that the factor $F_{\mathbf{k},\alpha,\beta} \propto \chi^2$ has the same dependence on the lattice constant a in both cases, i.e., $\chi^2 \propto a^{-3}$. On the other hand, in the 3D case we can associate the light-matter coupling to the volumetric density ρ, which in turn is related to the lattice constant through $\rho \propto a^{-3}$. In contrast, in the 2D lattice we have a light-matter constant dependent on a superficial density $\sigma \propto a^{-2}$ (it also depends on the cavity length L, which in contrast does not play any role in the dipole-dipole interaction term as expected). Therefore, for the 2D system, it can be clearly understood that the eventual softening of the transverse matter frequency is purely due to the dipolar interactions, independent of the coupling with the radiation field, which depends also on other parameters.

APPENDIX D: DERIVATION OF THE FULL HAMILTONIANS

In this section, we present the derivation of the full light-matter Hamiltonians in the 3D and 2D lattice, Eqs. (8) and (16) of the main text, respectively. In Appendix F, we proceed to introduce the diagonalization procedure for the full Hamiltonians and compare the results obtained with the results presented in the main paper, which instead follow a two-step Bogoliubov transformation (first on the matter subsystem and successively considering the interaction with the radiation field), thus demonstrating the equivalence of the two procedures.

1. 3D lattice

Let us consider the first system, which is composed of a three-dimensional bulk of atoms interacting with a quantized electromagnetic field. As usual, the vector potential $\mathbf{A}(\mathbf{r})$ and the bare photonic Hamiltonian H_{ph} are given by introducing radiation bosonic operators $a_{\mathbf{k},\lambda}$ for each mode $\mathbf{k}$ and polarization λ, leading to the plane-wave decomposition

$$\mathbf{A}(\mathbf{r}) = \sum_\lambda\sum_{\mathbf{k}} \mathcal{E}_k e^{i\mathbf{k}\cdot\mathbf{r}} a_{\mathbf{k},\lambda}\hat{\mathbf{e}}_\lambda + \text{H.c.}, \tag{D1}$$

$$H_{\text{ph}} = \sum_{\lambda,\mathbf{k}} \hbar\omega_k a_{\mathbf{k},\lambda}^\dagger a_{\mathbf{k},\lambda}, \tag{D2}$$

corresponding to Eqs. (1) and (2) of the main text.

We now can derive the full light-matter Hamiltonian in the multipolar gauge [49]. To this end, we apply to the Hamiltonian of the free electromagnetic field (D2) the unitary transformation U [21], defined in Eq. (7) of the main text as

$$U = \exp\left(\frac{i}{\hbar}\int \mathbf{A}(\mathbf{r}) \cdot \mathbf{P}(\mathbf{r}) d^3\mathbf{r}\right). \tag{D3}$$

As will be discussed below, this procedure ensures the gauge invariance of the treatment, according to the generalized definition of gauge invariance, consistent also for truncated Hilbert spaces [37]. For example, applying the transformation U to the matter Hamiltonian instead would recover the standard Coulomb gauge Hamiltonian within this bosonized framework [21]. Inserting the previous definitions for the vector potential Eq. (D1) and for the polarization density, $\mathbf{P}(\mathbf{r}) = \sum_n \mathbf{d}_n\delta(\mathbf{r} - \mathbf{R}_n)$, in this last equation, we obtain the transformation

$$U = \exp\left[\frac{i}{\hbar}\sum_{\lambda,\mathbf{k},n} \mathcal{E}_{\mathbf{k}}\left(e^{i\mathbf{k}\cdot\mathbf{R}_n} a_{\mathbf{k},\lambda} + e^{-i\mathbf{k}\cdot\mathbf{R}_n} a_{\mathbf{k},\lambda}^\dagger\right)\hat{\mathbf{e}}_\lambda \cdot \mathbf{d}_n\right]. \tag{D4}$$

A direct application of the transformation (D4) to the photonic Hamiltonian (D2) yields

$$U^\dagger H_{\rm ph} U = \sum_{\lambda,\mathbf{k}} \hbar\omega_k \left[a^\dagger_{\mathbf{k},\lambda} a_{\mathbf{k},\lambda} - \frac{i}{\hbar} \sum_n \mathcal{E}_{\mathbf{k}} \big(e^{i\mathbf{k}\cdot\mathbf{R}_n} a_{\mathbf{k},\lambda} - e^{-i\mathbf{k}\cdot\mathbf{R}_n} a^\dagger_{\mathbf{k},\lambda} \big) \hat{\mathbf{e}}_\lambda \cdot \mathbf{d}_n + \frac{1}{\hbar^2} \sum_{n,m} \mathcal{E}^2_{\mathbf{k}}\, e^{i\mathbf{k}\cdot(\mathbf{R}_n - \mathbf{R}_m)}\, \hat{\mathbf{e}}_\lambda \cdot \mathbf{d}_n\, \hat{\mathbf{e}}_\lambda \cdot \mathbf{d}_m \right]. \tag{D5}$$

We can now apply the two-level approximation (see Appendix A) and bosonize the system through the use of generalized Holstein-Primakoff transformations (see Appendix B), leading to the atomic and transformed photonic Hamiltonians, respectively:

$$H_{\rm A} = \hbar\omega_0 \sum_{\alpha,\mathbf{k}} b^\dagger_{\mathbf{k},\alpha} b_{\mathbf{k},\alpha}, \tag{D6}$$

$$\begin{aligned} U^\dagger H_{\rm ph} U = {} & \hbar \sum_{\lambda,\mathbf{k}} \omega_k a^\dagger_{\mathbf{k},\lambda} a_{\mathbf{k},\lambda} - i\hbar \sum_{\alpha,\lambda,\mathbf{k}} g_k \omega_k (a_{\mathbf{k},\lambda} - a^\dagger_{-\mathbf{k},\lambda})(b_{-\mathbf{k},\alpha} + b^\dagger_{\mathbf{k},\alpha}) e_{\lambda_\alpha} \\ & + \hbar \sum_{\alpha,\beta,\lambda,\mathbf{k}} g^2_k \omega_k (b_{-\mathbf{k},\alpha} + b^\dagger_{\mathbf{k},\alpha})(b_{\mathbf{k},\beta} + b^\dagger_{-\mathbf{k},\beta}) e_{\lambda_\alpha} e_{\lambda_\beta}, \end{aligned} \tag{D7}$$

where $g_k = \mathcal{E}_{\mathbf{k}} d\sqrt{N}/\hbar = \sqrt{d^2 N/2\hbar\epsilon_0\epsilon_m V\omega_k}$ and the $\hat{\mathbf{e}}_\alpha$ are a generic set of orthonormal basis vectors used as a basis for the decomposition of the dipole moments. Furthermore, we indicated for notation convenience $e_{\lambda_\alpha} \equiv \hat{\mathbf{e}}_\lambda \cdot \hat{\mathbf{e}}_\alpha$. The additional term describing the dipole-dipole interactions can be expressed (see Appendix C) in the thermodynamic limit as

$$H_{\rm dip} = \hbar \sum_{\alpha,\beta,\mathbf{k}} \chi^2 \omega_0 f_{\mathbf{k},\alpha,\beta} (b_{-\mathbf{k},\alpha} + b^\dagger_{\mathbf{k},\alpha})(b_{\mathbf{k},\beta} + b^\dagger_{-\mathbf{k},\beta}). \tag{D8}$$

Thus, the resulting bosonized matter Hamiltonian [Eq. (6) of the main paper] is given by

$$H_{\rm mat} = H_{\rm A} + H_{\rm dip} = \hbar\omega_0 \sum_{\alpha,\mathbf{k}} b^\dagger_{\mathbf{k},\alpha} b_{\mathbf{k},\alpha} + \hbar \sum_{\alpha,\beta,\mathbf{k}} \chi^2 \omega_0 f_{\mathbf{k},\alpha,\beta} (b_{-\mathbf{k},\alpha} + b^\dagger_{\mathbf{k},\alpha})(b_{\mathbf{k},\beta} + b^\dagger_{-\mathbf{k},\beta}). \tag{D9}$$

The total Hamiltonian in the multipolar gauge is then given by

$$\begin{aligned} H = {} & \hbar \sum_{\lambda,\mathbf{k}} \omega_k a^\dagger_{\mathbf{k},\lambda} a_{\mathbf{k},\lambda} + \hbar\omega_0 \sum_{\alpha,\mathbf{k}} b^\dagger_{\mathbf{k},\alpha} b_{\mathbf{k},\alpha} - i\hbar \sum_{\alpha,\lambda,\mathbf{k}} g_k \omega_k (a_{\mathbf{k},\lambda} - a^\dagger_{-\mathbf{k},\lambda})(b_{-\mathbf{k},\alpha} + b^\dagger_{\mathbf{k},\alpha}) e_{\lambda_\alpha} \\ & + \hbar \sum_{\alpha,\beta,\lambda,\mathbf{k}} g^2_k \omega_k (b_{-\mathbf{k},\alpha} + b^\dagger_{\mathbf{k},\alpha})(b_{\mathbf{k},\beta} + b^\dagger_{-\mathbf{k},\beta}) e_{\lambda_\alpha} e_{\lambda_\beta} + \hbar \sum_{\alpha,\beta,\mathbf{k}} \chi^2 \omega_0 f_{\mathbf{k},\alpha,\beta} (b_{-\mathbf{k},\alpha} + b^\dagger_{\mathbf{k},\alpha})(b_{\mathbf{k},\beta} + b^\dagger_{-\mathbf{k},\beta}). \end{aligned} \tag{D10}$$

The first two terms in Eq. (D10) represent the free radiation and matter fields, the third and the fourth are the transverse interactions between light and matter, while the last one represents the dipole-dipole electrostatic interactions. Performing a Bogoliubov diagonalization on the matter subsystem (see Appendix E), Eq. (D10) reduces to Eq. (8) of the main text.

We observe that, in the previous calculations, from Eq. (D3) to Eq. (D7), we *first* performed the transformation U and *subsequently* the two-level approximation, followed by the bosonization procedure, as made clear by the presence of the full dipoles $\mathbf{d}_n$ (no two-level approximation has been performed yet) in Eq. (D2). On the other hand, consistent results in the multipolar gauge can also be derived if we *first* perform the two-level approximation and the bosonization directly in the definition of U in Eq. (D3), and *after* apply this transformation to the photonic Hamiltonian Eq. (D2) [21]. In fact, after some algebraic manipulations, Eq. (D3) in terms of the bosonic operators becomes

$$U = \exp\left[i \sum_{\alpha,\lambda,\mathbf{k}} g_k (a_{\mathbf{k},\lambda} + a^\dagger_{-\mathbf{k},\lambda})(b_{-\mathbf{k},\alpha} + b^\dagger_{\mathbf{k},\alpha}) e_{\lambda_\alpha} \right]. \tag{D11}$$

Applying such a transformation to the photonic Hamiltonian Eq. (D2), then the same Hamiltonian Eq. (D7) is reached, thus demonstrating the equivalence of the two approaches.

One advantage of the latter approach is that the resulting total light-matter Hamiltonian in the multipolar gauge H [Eq. (D10)] is related to the corresponding Coulomb gauge Hamiltonian $H_{\rm C}$ by the very same unitary transformation U as $H_{\rm C} = UHU^\dagger$ (see Ref. [21]), ensuring the gauge invariance of the treatment. Hence, we have

$$\begin{aligned} H_{\rm C} &= U(H_{\rm A} + U^\dagger H_{\rm ph} U + H_{\rm dip})U^\dagger \\ &= UH_{\rm A}U^\dagger + H_{\rm ph} + H_{\rm dip}, \end{aligned} \tag{D12}$$

where in the last equality we utilized the property $[U, H_{\rm dip}] = 0$, which aligns with the physical interpretation that the electrostatic contribution remains unchanged across different gauges. The term $UH_{\rm A}U^\dagger$ recovers the usual minimal coupling replacement, typical of the Coulomb gauge light-matter Hamiltonian. Equations (D12) and (D10), being related by the unitary transformation U, yield identical dispersion relations for both the longitudinal and transverse sectors. This consistency highlights the gauge invariance of our results.

2. 2D lattice

Let us now consider the 2D system, composed of a two-dimensional layer of atoms, identified as the xy plane, embedded in an ideal cavity. This planar configuration

naturally induces a decomposition of the vector potential as

$$A(\mathbf{r})=\sum_{\lambda,\mathbf{k}_\parallel}\sum_{k_z>0}\mathcal{E}_k e^{i\mathbf{k}_\parallel\cdot\mathbf{r}_\parallel}\left(e^{ik_z z}a_{l,\mathbf{k}_\parallel,k_z,\lambda}+e^{-ik_z z}a_{r,\mathbf{k}_\parallel,k_z,\lambda}\right)\hat{\mathbf{e}}_\lambda+\text{H.c.}, \tag{D13}$$

where $\mathbf{k}_\parallel$ is the in-plane discrete component of the wave vector, S being the corresponding quantization surface, while k_z is its orthogonal component quantized by the length of the cavity L, as already stated in the main text. In this expression, $\mathcal{E}_k=\sqrt{\hbar/2\epsilon_0\epsilon_m\omega_k SL}$ and $\omega_k=v\sqrt{\mathbf{k}_\parallel^2+k_z^2}$. Moreover, we introduced the left and right creation operators $a_{l(r),\mathbf{k}_\parallel,k_z,\lambda}\equiv a_{\mathbf{k}_\parallel,\pm k_z,\lambda}$, where the index $l\,(r)$ is associated with the $+(-)$ sign. If we consider the case of normal incidence $\mathbf{k}_\parallel=\mathbf{0}$, and thus $\mathbf{k}=k_z\hat{\mathbf{z}}$, Eq. (D13) considerably simplifies given that the two polarization vectors $\hat{\mathbf{e}}_\lambda$ now lie in the xy plane and the bosonic operators become independent on $\mathbf{k}_\parallel$, i.e., $a_{l(r),k_z,\lambda}\equiv a_{l(r),\mathbf{k}_\parallel=\mathbf{0},k_z,\lambda}$. Defining even and odd radiation modes operators, $a_{e(o),k_z,\lambda}=(a_{l,k_z,\lambda}\pm a_{r,k_z,\lambda})/\sqrt{2}$, the Hamiltonian of the free electromagnetic field can be written as in Eq. (14) of the main text:

$$H_{\text{ph}}=\sum_\lambda\sum_{j=e,o}\sum_{k_z>0}\hbar\omega_{k_z}a^\dagger_{j,k_z,\lambda}a_{j,k_z,\lambda}. \tag{D14}$$

For the matter subsystem, we follow an analogous procedure to the 3D lattice of dipoles. We first perform the two-level approximation, taking into account the dipole orientations, and successively construct two-dimensional collective bosonic operators $b_{\mathbf{k}_\parallel}$. Considering only radiation modes with wave vectors orthogonal to the 2D lattice surface (normal incidence), implying $\mathbf{k}_\parallel=0$, the final atomic Hamiltonian reads

$$H_{\text{A}}=\hbar\omega_0\sum_\alpha b^\dagger_\alpha b_\alpha. \tag{D15}$$

We now calculate the transformation U, analogous to Eq. (D3), for such a system, yielding

$$U=\exp\left[\frac{i}{\hbar}\sum_{\lambda,n}\sum_{k_z>0}\sqrt{2}\mathcal{E}_{k_z}\left(a_{e,k_z,\lambda}+a^\dagger_{e,k_z,\lambda}\right)\hat{\mathbf{e}}_\lambda\cdot\mathbf{d}_n\right], \tag{D16}$$

where, again, only modes perpendicular to the planar surface have been considered. Applying this transformation to the photonic Hamiltonian Eq. (D14), we obtain

$$\begin{aligned}U^\dagger H_{\text{ph}}U=\sum_{\lambda,k_z>0}\hbar\omega_{k_z}\Bigg[&\sum_{j=e,o}a^\dagger_{j,k_z,\lambda}a_{j,k_z,\lambda}\\&-\frac{i}{\hbar}\sum_n\sqrt{2}\mathcal{E}_{k_z}\left(a_{e,k_z,\lambda}-a^\dagger_{e,k_z,\lambda}\right)\hat{\mathbf{e}}_\lambda\cdot\mathbf{d}_n\\&+\frac{1}{\hbar^2}\sum_{n,m}2\mathcal{E}^2_{k_z}\,\hat{\mathbf{e}}_\lambda\cdot\mathbf{d}_n\,\hat{\mathbf{e}}_\lambda\cdot\mathbf{d}_m\Bigg].\end{aligned} \tag{D17}$$

Therefore, after the bosonization in the thermodynamic limit, the full light-matter Hamiltonian, considering the addition of the dipole-dipole interactions in a planar layer Eq. (C9), is given by

$$\begin{aligned}H=&\hbar\sum_{\lambda,k_z>0}\omega_{k_z}\left(a^\dagger_{e,k_z,\lambda}a_{e,k_z,\lambda}+a^\dagger_{o,k_z,\lambda}a_{o,k_z,\lambda}\right)+\hbar\omega_0\sum_\alpha b^\dagger_\alpha b_\alpha\\&-i\hbar\sum_{\alpha,\lambda,k_z>0}g_{k_z}\omega_{k_z}\left(a_{e,k_z,\lambda}-a^\dagger_{e,k_z,\lambda}\right)(b_\alpha+b^\dagger_\alpha)e_{\lambda_\alpha}\\&+\hbar\sum_{\alpha,\beta,\lambda,k_z>0}g^2_{k_z}\omega_{k_z}(b_\alpha+b^\dagger_\alpha)(b_\beta+b^\dagger_\beta)e_{\lambda_\alpha}e_{\lambda_\beta}\\&+\hbar\sum_{\alpha,\beta}\chi^2\omega_0 f_{\mathbf{z},\alpha,\beta}(b_\alpha+b^\dagger_\alpha)(b_\beta+b^\dagger_\beta),\end{aligned} \tag{D18}$$

where $g_k=\sqrt{d^2N/\hbar\epsilon_0\epsilon_m SL\omega_{k_z}}$. Equation (D18) is the same as Eq. (16) of the main text.

APPENDIX E: BOGOLIUBOV DIAGONALIZATION OF THE MATTER HAMILTONIAN

As discussed in the main paper, we can first diagonalize the matter Hamiltonian H_{mat} using the Bogoliubov diagonalization procedure. In particular, the Hamiltonian that we wish to diagonalize is of the form given by Eq. (D9). The resulting Bogoliubov matrix associated to mode $\mathbf{k}$ and orientation α, in the basis $b_{\mathbf{k},\alpha}, b^\dagger_{-\mathbf{k},\alpha}$, is

$$\begin{pmatrix}\omega_0+2\chi^2\omega_0 f_{\mathbf{k},\alpha,\beta} & 2\chi^2\omega_0 f_{\mathbf{k},\alpha,\beta}\\ -2\chi^2\omega_0 f_{\mathbf{k},\alpha,\beta} & -\omega_0-2\chi^2\omega_0 f_{\mathbf{k},\alpha,\beta}\end{pmatrix}. \tag{E1}$$

The resulting eigenvalues are $\tilde{\omega}_{\mathbf{k},\alpha}=\omega_0\sqrt{1+4\eta^2 f_{\mathbf{k},\alpha,\alpha}}$, and the corresponding eigenvectors are

$$c_{\mathbf{k},\alpha}=\frac{2\chi^2\omega_0 f_{\mathbf{k},\alpha,\alpha}}{\sqrt{\mathcal{N}}}b_{\mathbf{k},\alpha}-\frac{\tilde{\omega}_{\mathbf{k},\alpha}-\omega_0-2\chi^2\omega_0 f_{\mathbf{k},\alpha,\alpha}}{\sqrt{\mathcal{N}}}b^\dagger_{-\mathbf{k},\alpha}, \tag{E2}$$

and its Hermitian conjugate ($c^\dagger_{\mathbf{k},\alpha}$), where $\mathcal{N}=(\tilde{\omega}_{\mathbf{k},\alpha}-\omega_0)(\omega_0+2\chi^2\omega_0 f_{\mathbf{k},\alpha,\alpha}-\tilde{\omega}_{\mathbf{k},\alpha})$ is the normalization factor such that $[c_{\mathbf{k},\alpha},c^\dagger_{\mathbf{k}',\alpha'}]=\delta_{\mathbf{k},\mathbf{k}'}\delta_{\alpha,\alpha'}$.

APPENDIX F: CALCULATION OF THE DISPERSION RELATIONS

The dispersion relations can be calculated through the use of a Hopfield-Bogoliubov diagonalization of the total system Hamiltonian, e.g., Hamiltonian (D10) for the 3D lattice or (D18) for the 2D case, or equivalently by a two-step diagonalization as presented in the main paper. In this section we will follow the first procedure, and verify the equivalence of the results derived by the two approaches.

1. Calculation of the dispersion relations for the 3D lattice

In this subsection we focus on the calculations regarding the 3D arrangement. First, from Hamiltonian Eq. (D10), let us

evaluate the following commutators:

$$[a_{\mathbf{k},\lambda}, H] = \hbar\omega_k a_{\mathbf{k},\lambda} + i\hbar g_k\omega_k \sum_\alpha (b^\dagger_{-\mathbf{k},\alpha} + b_{\mathbf{k},\alpha}) e_{\lambda_\alpha}, \tag{F1}$$

$$[a^\dagger_{\mathbf{k},\lambda}, H] = -\hbar\omega_k a^\dagger_{\mathbf{k},\lambda} + i\hbar g_k\omega_k \sum_\alpha (b^\dagger_{\mathbf{k},\alpha} + b_{-\mathbf{k},\alpha}) e_{\lambda_\alpha}, \tag{F2}$$

$$[b_{\mathbf{k},\alpha}, H] = \hbar\omega_0 b_{\mathbf{k},\alpha} + i\hbar g_k\omega_k \sum_\lambda (a^\dagger_{-\mathbf{k},\lambda} - a_{\mathbf{k},\lambda}) e_{\lambda_\alpha} + 2\hbar g_k^2\omega_k \sum_\beta \left[\sum_\lambda e_{\lambda_\beta} e_{\lambda_\alpha} + f_{\mathbf{k},\alpha,\beta}\right](b^\dagger_{-\mathbf{k},\beta} + b_{\mathbf{k},\beta}), \tag{F3}$$

$$[b^\dagger_{\mathbf{k},\alpha}, H] = -\hbar\omega_0 b^\dagger_{\mathbf{k},\alpha} - i\hbar g_k\omega_k \sum_\lambda (a^\dagger_{\mathbf{k},\lambda} - a_{-\mathbf{k},\lambda}) e_{\lambda_\alpha} - 2\hbar g_k^2\omega_k \sum_\beta \left[\sum_\lambda e_{\lambda_\beta} e_{\lambda_\alpha} + f_{\mathbf{k},\alpha,\beta}\right](b^\dagger_{\mathbf{k},\beta} + b_{-\mathbf{k},\beta}). \tag{F4}$$

Thus, writing the Heisenberg equations and transforming to the frequency-domain Fourier space, we have

$$\hbar(\Omega - \omega_k)\mathcal{A}_{\mathbf{k},\lambda} = i\hbar g_k\omega_k \sum_\alpha (\mathcal{B}^\dagger_{-\mathbf{k},\alpha} + \mathcal{B}_{\mathbf{k},\alpha}) e_{\lambda_\alpha}. \tag{F5}$$

$$\hbar(\Omega + \omega_k)\mathcal{A}^\dagger_{-\mathbf{k},\lambda} = i\hbar g_k\omega_k \sum_\alpha (\mathcal{B}^\dagger_{-\mathbf{k},\alpha} + \mathcal{B}_{\mathbf{k},\alpha}) e_{\lambda_\alpha}, \tag{F6}$$

$$\hbar(\Omega - \omega_0)\mathcal{B}_{\mathbf{k},\alpha} = i\hbar g_k\omega_k \sum_\lambda (\mathcal{A}^\dagger_{-\mathbf{k},\lambda} - \mathcal{A}_{\mathbf{k},\lambda}) e_{\lambda_\alpha} + 2\hbar g_k^2\omega_k \sum_\beta \left[\sum_\lambda e_{\lambda_\beta} e_{\lambda_\alpha} + f_{\mathbf{k},\alpha,\beta}\right](\mathcal{B}^\dagger_{-\mathbf{k},\beta} + \mathcal{B}_{\mathbf{k},\beta}), \tag{F7}$$

$$\hbar(\Omega + \omega_0)\mathcal{B}^\dagger_{-\mathbf{k},\alpha} = -i\hbar g_k\omega_k \sum_\lambda (\mathcal{A}^\dagger_{-\mathbf{k},\lambda} - \mathcal{A}_{\mathbf{k},\lambda}) e_{\lambda_\alpha} - 2\hbar g_k^2\omega_k \sum_\beta \left[\sum_\lambda e_{\lambda_\beta} e_{\lambda_\alpha} + f_{\mathbf{k},\alpha,\beta}\right](\mathcal{B}^\dagger_{-\mathbf{k},\beta} + \mathcal{B}_{\mathbf{k},\beta}), \tag{F8}$$

where $\mathcal{A}_{\mathbf{k},\lambda}(\Omega)$ and $\mathcal{B}_{\mathbf{k},\lambda}(\Omega)$ are the Fourier transforms of the operators $a_{\mathbf{k},\lambda}(t)$ and $b_{\mathbf{k},\lambda}(t)$, respectively (the dependencies on time or frequency are omitted for simplicity).

Solving this system we can derive self-consistent equations for the transverse and longitudinal sectors. We consider here for simplicity the dipole basis used for the decomposition $\mathbf{e}_\alpha$ coincident with the basis induced by radiation field and successively select the transverse and longitudinal components, respectively, thus obtaining

$$\frac{\omega_{\mathbf{k}}^2}{\Omega_\perp^2} = 1 + \frac{4g_k^2\omega_k\omega_0}{\omega_0^2 + 4g_k^2\omega_k\omega_0 f_{\mathbf{k}}^\perp - \Omega_\perp^2}, \tag{F9}$$

$$\Omega_\parallel^2 = \omega_0^2 + 4g_k^2\omega_k\omega_0 f_{\mathbf{k}}^\parallel, \tag{F10}$$

where $f_{\mathbf{k}}^\perp$ and $f_{\mathbf{k}}^\parallel$ represent the transverse and longitudinal components of $f_{\mathbf{k},\alpha,\beta}$, respectively. For isotropic systems, in the long-wavelength approximation $f_{\mathbf{k}}^\perp = -1/3$ and $f_{\mathbf{k}}^\parallel = 2/3$.

If we introduce a renormalized matter frequency defined, as in the main paper, by $\tilde{\omega}_{\mathbf{k},\alpha} = \omega_0\sqrt{1 + 4\eta^2 f_{\mathbf{k},\alpha,\alpha}}$, the dispersion relation for the transverse sector (F9) becomes equivalent to the one derived by a Hopfield model with renormalized factors

$$\frac{\omega_{\mathbf{k}}^2}{\Omega_\perp^2} = 1 + \frac{4g_k'^2\omega_k\tilde{\omega}_{\mathbf{k}}^\perp}{\tilde{\omega}_{\mathbf{k}}^{\perp 2} - \Omega_\perp^2}, \tag{F11}$$

where $g_k' = g_k\sqrt{\omega_0/\tilde{\omega}_{\mathbf{k}}^\perp}$ is the normalized coupling and $\tilde{\omega}_{\mathbf{k}}^\perp = \omega_0\sqrt{1 + 4\eta^2 f_{\mathbf{k}}^\perp}$ is the normalized transverse frequency. Introducing the coupling constant $\eta = \sqrt{d^2N/2\hbar\epsilon_m V\omega_0}$, the previous dispersion relation can be written as

$$\frac{\omega_{\mathbf{k}}^2}{\Omega_\perp^2} = 1 + \frac{4\eta^2\omega_0^2}{\omega_0^2 + 4\eta^2\omega_0^2 f_{\mathbf{k}}^\perp - \Omega_\perp^2} = 1 + \frac{4\eta'^2\tilde{\omega}_{\mathbf{k}}^{\perp 2}}{\tilde{\omega}_{\mathbf{k}}^{\perp 2} - \Omega_\perp^2}, \tag{F12}$$

where we defined the renormalized coupling $\eta' = \eta\,\omega_0/\tilde{\omega}_{\mathbf{k}}^\perp$ in order to reduce the dispersion relation to a Hopfield-like one. Equation (F12) coincides with Eq. (10) of the main paper, thus demonstrating the equivalence between this diagonalization procedure of the full Hamiltonian and the two-step diagonalization introduced in the main paper. The coupling constant η is particularly useful in the evaluation of the experimental results, since it corresponds to the ratio between the Rabi frequency Ω_R (which in turn is half the splitting between the level anticrossing) and the matter frequency, i.e., $\eta = \Omega_R/\omega_0$. Analogously, the normalized coupling constant η' is related to the normalized matter frequency through $\eta' = \Omega_R/\tilde{\omega}_{\mathbf{k}}^\perp$. Figure 4 shows an example of typical dispersion curves, in which all the main physical dispersions are illustrated.

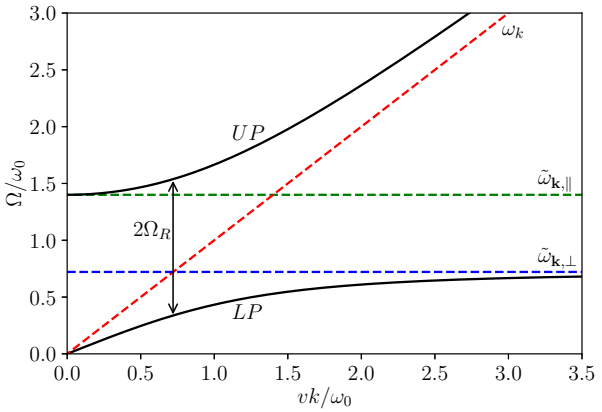

FIG. 4. Dispersion curves of a renormalized Hopfield-like model in Eq. (F12), calculated with $\eta = 0.6$.

2. Calculation of the dispersion relations for the 2D lattice

In this subsection, we apply the same diagonalization procedure to the Hamiltonian of the 2D lattice Eq. (D18). Following the same steps of the previous subsection, we can write the Heisenberg equations of motion in the Fourier space:

$$(\Omega-\omega_k)\;\; \mathcal{A}_{e,k_z,\lambda} = ig_k\omega_k\sum_\alpha(\mathcal{B}^\dagger_\alpha+\mathcal{B}_\alpha)e_{\lambda_\alpha}, \tag{F13}$$

$$(\Omega+\omega_k)\;\; \mathcal{A}^\dagger_{e,k_z,\lambda} = ig_k\omega_k\sum_\alpha(\mathcal{B}^\dagger_\alpha+\mathcal{B}_\alpha)e_{\lambda_\alpha}, \tag{F14}$$

$$(\Omega-\omega_0)\;\; \mathcal{B}_\alpha = ig_k\omega_k\sum_{\lambda,k_z>0}\left(\mathcal{A}^\dagger_{e,k_z,\lambda}-\mathcal{A}_{e,k_z,\lambda}\right)e_{\lambda_\alpha}+2\sum_\beta\left[\sum_\lambda e_{\lambda_\beta}e_{\lambda_\alpha}\sum_{k_z>0}g_k^2\omega_k+\chi^2\omega_0 f_{\mathbf{z},\alpha,\beta}\right](\mathcal{B}^\dagger_\beta+\mathcal{B}_\beta), \tag{F15}$$

$$(\Omega+\omega_0)\;\; \mathcal{B}^\dagger_\alpha = -ig_k\omega_k\sum_{\lambda,k_z>0}\left(\mathcal{A}^\dagger_{e,k_z,\lambda}-\mathcal{A}_{e,k_z,\lambda}\right)e_{\lambda_\alpha}-2\sum_\beta\left[\sum_\lambda e_{\lambda_\beta}e_{\lambda_\alpha}\sum_{k_z>0}g_k^2\omega_k+\chi^2\omega_0 f_{\mathbf{z},\alpha,\beta}\right](\mathcal{B}^\dagger_\beta+\mathcal{B}_\beta), \tag{F16}$$

where, as usual, $\mathcal{A}_{e,k_z,\lambda}(\Omega)$ and $\mathcal{B}_\alpha(\Omega)$ are the Fourier transforms of the operators $a_{e,k_z,\lambda}(t)$ and $b_\alpha(t)$. Notice that the odd-mode radiation operators $a_{o,k_z,\lambda}(t)$ have a trivial dynamics, given that they do not couple with the radiation field, and thus are irrelevant in this calculation.

Solving this system, we obtain the dispersion relations for the transverse sector reported in the main paper:

$$\frac{\omega_0^2-\Omega_\perp^2}{2\omega_0} = 2\left[\sum_{k_z>0}\frac{g_k^2\omega_k\Omega_\perp^2}{\omega_{k_z}^2-\Omega_\perp^2}-\chi^2\omega_0 f_{\mathbf{z}}^\perp\right]. \tag{F17}$$

Introducing the coupling constant $\eta = g_k\sqrt{\omega_k/\omega_0}$, and by defining the renormalized transverse matter frequency $\tilde{\omega}^\perp = \omega_0\sqrt{1+4\chi^2 f_{\mathbf{z}}^\perp}$, as in the main paper, we can rewrite the dispersion relations as

$$\frac{\Omega_\perp^2-\tilde{\omega}^{\perp^2}}{2\tilde{\omega}^\perp}+2\eta'^2\tilde{\omega}^\perp\sum_{k_z>0}\frac{\Omega_\perp^2}{\omega_{k_z}^2-\Omega_\perp^2} = 0, \tag{F18}$$

which coincides with Eq. (18) of the main paper.

APPENDIX G: DISPERSION RELATIONS BEYOND THE PHASE TRANSITION

In this section we derive the dispersion relations for Hamiltonian (D10) beyond the phase transition. Such a Hamiltonian has to be modified accordingly for coupling strength greater than the critical value η_c, given the predicted macroscopic occupation of the fields in this new phase. In order to correctly describe this phenomenon, we shift the bosonic radiation and matter mode operators as [32]

$$a_{\mathbf{k},\lambda} = \tilde{a}_{\mathbf{k},\lambda}-iA_{\mathbf{k},\lambda}, \tag{G1}$$

$$b_{\mathbf{k},\alpha} = \tilde{b}_{\mathbf{k},\alpha}+B_{\mathbf{k},\alpha}, \tag{G2}$$

where the real parameters $A_{\mathbf{k},\lambda}$ and $B_{\mathbf{k},\alpha}$ are linked to the macroscopic mean field mode occupation. Thus, we expect them to be zero in the normal phase and of order $O(\sqrt{N})$ beyond the phase transition. After substituting these relations into Eq. (D10), expanding the square root contribution in the Holstein-Primakoff procedure, and retaining only the terms up to second order, the resulting superradiant phase Hamiltonian in the multipolar gauge, in the thermodynamic limit, is given by

$$\begin{aligned}H =\;& \hbar\sum_{\lambda,\mathbf{k}}\omega_k\tilde{a}^\dagger_{\mathbf{k},\lambda}\tilde{a}_{\mathbf{k},\lambda}+\hbar\sum_{\alpha,\mathbf{k}}\left[\omega_0+2\frac{\tilde{g}_k}{\tilde{N}_k}\omega_k\sum_{\lambda,\beta}A_{\mathbf{k},\lambda}B_{\mathbf{k},\beta}e_{\lambda_\beta}-4\frac{\tilde{g}_k^2}{\tilde{N}_k}\omega_k\tilde{f}_{\mathbf{k},\beta,\gamma}\sum_{\beta,\gamma}B_{\mathbf{k},\beta}B_{\mathbf{k},\gamma}\right]\tilde{b}^\dagger_{\mathbf{k},\alpha}\tilde{b}_{\mathbf{k},\alpha}\\ &-i\hbar\sum_{\lambda,\mathbf{k}}\left[2\tilde{g}_k\omega_k\sum_\alpha B_{\mathbf{k},\alpha}e_{\lambda_\alpha}-\omega_k A_{\mathbf{k},\lambda}\right](\tilde{a}_{\mathbf{k},\lambda}-\tilde{a}^\dagger_{-\mathbf{k},\lambda})\\ &-\hbar\sum_{\alpha,\mathbf{k}}\left[2\tilde{g}_k\omega_k\sum_\lambda A_{\mathbf{k},\lambda}e_{\lambda_\alpha}-\left(\omega_0+2\frac{\tilde{g}_k}{\tilde{N}_k}\omega_k\sum_{\lambda,\beta}A_{\mathbf{k},\lambda}B_{\mathbf{k},\beta}e_{\lambda_\beta}\right)B_{\mathbf{k},\alpha}\right.\end{aligned}$$

$$
\begin{aligned}
&+4\tilde{g}_k^2\omega_k\left(\frac{B_{\mathbf{k},\alpha}}{\tilde{N}_k}\sum_{\beta,\gamma}B_{\mathbf{k},\beta}B_{\mathbf{k},\gamma}\tilde{f}_{\mathbf{k},\beta,\gamma}-\sum_{\beta}B_{\mathbf{k},\beta}\tilde{f}_{\mathbf{k},\alpha,\beta}\right)\Bigg](\tilde{b}_{\mathbf{k},\alpha}+\tilde{b}^\dagger_{-\mathbf{k},\alpha})\\
&-i\hbar\sum_{\alpha,\lambda,\mathbf{k}}\left[\frac{\tilde{g}_k}{\tilde{N}_k}\omega_k\left(\tilde{N}_k e_{\lambda_\alpha}-B_{\mathbf{k},\alpha}\sum_{\beta}B_{\mathbf{k},\beta}e_{\lambda_\beta}\right)\right](\tilde{a}_{\mathbf{k},\lambda}-\tilde{a}^\dagger_{-\mathbf{k},\lambda})(\tilde{b}_{-\mathbf{k},\alpha}+\tilde{b}^\dagger_{\mathbf{k},\alpha})\\
&+\hbar\sum_{\alpha,\beta,\lambda,\mathbf{k}}\Bigg[\frac{\tilde{g}_k}{2\tilde{N}_k^2}\omega_k A_{\mathbf{k},\lambda}B_{\mathbf{k},\alpha}\left(2\tilde{N}_k e_{\lambda_\beta}+B_{\mathbf{k},\beta}\sum_{\gamma}B_{\mathbf{k},\gamma}e_{\lambda_\gamma}\right)\\
&\qquad+\frac{\tilde{g}_k^2}{\tilde{N}_k}\omega_k\left(\tilde{N}_k\tilde{f}_{\mathbf{k},\alpha,\beta}-4B_{\mathbf{k},\alpha}\sum_{\gamma}\tilde{f}_{\mathbf{k},\beta,\gamma}B_{\mathbf{k},\gamma}\right)\Bigg](\tilde{b}_{-\mathbf{k},\alpha}+\tilde{b}^\dagger_{\mathbf{k},\alpha})(\tilde{b}_{\mathbf{k},\beta}+\tilde{b}^\dagger_{-\mathbf{k},\beta}),
\end{aligned}
\tag{G3}
$$

where $\tilde{g}_k = g_k\sqrt{\tilde{N}_k/N}$, $\tilde{N}_k = N-\sum_\alpha B^2_{\mathbf{k},\alpha}$ and $\tilde{f}_{\mathbf{k},\alpha,\beta} = \sum_\lambda e_{\lambda_\alpha}e_{\lambda_\beta}+f_{\mathbf{k},\alpha,\beta}$. The parameters $A_{\mathbf{k},\lambda}$ and $B_{\mathbf{k},\alpha}$, at equilibrium, are fixed by the stationary condition of the energy functional, which in turn is equivalent to imposing the vanishing of the linear terms in the bosonic operators. Thus, for each mode $\mathbf{k}$, we have the resulting system of two coupled equations in the two parameters $A_{\mathbf{k},\lambda}$ and $B_{\mathbf{k},\alpha}$:

$$
\begin{aligned}
&2\tilde{g}_k\omega_k\sum_{\alpha}B_{\mathbf{k},\alpha}e_{\lambda_\alpha}-\omega_k A_{\mathbf{k},\lambda}=0,\\
&2\tilde{g}_k\omega_k\left(\sum_{\lambda}A_{\mathbf{k},\lambda}e_{\lambda_\alpha}-\frac{B_{\mathbf{k},\alpha}}{\tilde{N}_k}\sum_{\lambda,\beta}A_{\mathbf{k},\lambda}B_{\mathbf{k},\beta}e_{\lambda_\beta}\right)+4\tilde{g}_k^2\omega_k\left(\frac{B_{\mathbf{k},\alpha}}{\tilde{N}_k}\sum_{\beta,\gamma}B_{\mathbf{k},\beta}B_{\mathbf{k},\gamma}\tilde{f}_{\mathbf{k},\beta,\gamma}-\sum_{\beta}B_{\mathbf{k},\beta}\tilde{f}_{\mathbf{k},\alpha,\beta}\right)-\omega_0 B_{\mathbf{k},\alpha}=0.
\end{aligned}
\tag{G4}
$$

We now focus our attention on the transverse mode solutions, since those are the ones coupling with the radiation field. This system of Eqs. (G4) admits, beside the trivial solution $A_{\mathbf{k},\lambda}=B_{\mathbf{k},\alpha}=0$ corresponding to the normal phase where no condensation occurs, a nontrivial solution which is defined by the conditions for the parameters

$$
\sum_{\alpha}B^2_{\mathbf{k},\alpha}=\frac{N}{2}\left(1+\frac{1}{4\eta^2 f^\perp_{\mathbf{k}}}\right),
\tag{G5}
$$

$$
A_{\mathbf{k},\lambda}=2\tilde{g}_k\sum_{\alpha}B_{\mathbf{k},\alpha}e_{\lambda_\alpha}.
\tag{G6}
$$

Inserting these values of the parameters in (G3), we obtain the Hamiltonian describing the condensed phase:

$$
\begin{aligned}
H_{\mathrm{CP}}=&\,\hbar\sum_{\lambda,\mathbf{k}}\omega_k\tilde{a}^\dagger_{\mathbf{k},\lambda}\tilde{a}_{\mathbf{k},\lambda}+\hbar\sum_{\alpha,\mathbf{k}}\omega_0\frac{1-4\eta^2 f^\perp_{\mathbf{k}}}{2}\tilde{b}^\dagger_{\mathbf{k},\alpha}\tilde{b}_{\mathbf{k},\alpha}\\
&-i\hbar\sum_{\alpha,\lambda,\mathbf{k}}\left[\frac{\tilde{g}_k}{\tilde{N}_k}\omega_k\left(\tilde{N}_k e_{\lambda_\alpha}-B_{\mathbf{k},\alpha}\sum_{\beta}B_{\mathbf{k},\beta}e_{\lambda_\beta}\right)\right](\tilde{a}_{\mathbf{k},\lambda}-\tilde{a}^\dagger_{-\mathbf{k},\lambda})(\tilde{b}_{-\mathbf{k},\alpha}+\tilde{b}^\dagger_{\mathbf{k},\alpha})\\
&+\hbar\sum_{\alpha,\mathbf{k}}\eta^2\omega_0(1+f^\perp_{\mathbf{k}})\frac{4\eta^2 f^\perp_{\mathbf{k}}-1}{8\eta^2 f^\perp_{\mathbf{k}}}(\tilde{b}_{-\mathbf{k},\alpha}+\tilde{b}^\dagger_{\mathbf{k},\alpha})(\tilde{b}_{\mathbf{k},\alpha}+\tilde{b}^\dagger_{-\mathbf{k},\alpha})\\
&+\hbar\sum_{\alpha,\beta,\mathbf{k}}\frac{\eta^2\omega_0}{N}\left[\frac{12\eta^2 f^\perp_{\mathbf{k}}-1}{4\eta^2 f^\perp_{\mathbf{k}}-1}-4(1+f^\perp_{\mathbf{k}})\right]B_{\mathbf{k},\alpha}B_{\mathbf{k},\beta}(\tilde{b}_{-\mathbf{k},\alpha}+\tilde{b}^\dagger_{\mathbf{k},\alpha})(\tilde{b}_{\mathbf{k},\beta}+\tilde{b}^\dagger_{-\mathbf{k},\beta}).
\end{aligned}
\tag{G7}
$$

Calculating the dispersion relations induced by this Hamiltonian (G7) as outlined in Appendix F, we obtain the following dispersion relation for the transverse mode solutions:

$$
\frac{\omega^2_{\mathbf{k}}}{\Omega^2_\perp}=1+\frac{\omega_0^2/f^\perp_{\mathbf{k}}}{\omega_0^2\left(1-16\eta^4 {f^\perp_{\mathbf{k}}}^2\right)+\Omega^2_\perp}.
\tag{G8}
$$

Therefore, combining Eqs. (F12) and (G8) for the dispersion relations before and after the QPT, we obtain (see Fig. 5)

$$\begin{cases} \dfrac{\omega_{\mathbf{k}}^2}{\Omega_\perp^2} = 1 + \dfrac{4\eta^2\omega_0^2}{\omega_0^2\left(1+4\eta^2 f_{\mathbf{k}}^\perp\right) - \Omega_\perp^2} & \eta < \eta_c, \\ \dfrac{\omega_{\mathbf{k}}^2}{\Omega_\perp^2} = 1 + \dfrac{\omega_0^2/f_{\mathbf{k}}^\perp}{\omega_0^2\left(1-16\eta^4 {f_{\mathbf{k}}^\perp}^2\right) + \Omega_\perp^2} & \eta > \eta_c. \end{cases} \tag{G9}$$

We can now investigate the ground state condensation occurring after the QPT. This study can be conduced in terms of mean mode occupation of the physical fields. In particular, the electric displacement field $\mathbf{D}(\mathbf{r})$ can be easily demonstrated to have a mean mode occupation, $\langle D_{\mathbf{k}}\rangle$, which equals to the mean transverse polarization field $\langle P_{\mathbf{k}}^\perp\rangle$. In the multipolar gauge, we have the radiation field canonical momentum $\mathbf{\Pi}(\mathbf{r}) = -\mathbf{D}(\mathbf{r})$, which leads to

$$\mathbf{D}(\mathbf{r}) = -\mathbf{\Pi}(\mathbf{r}) = i\epsilon_m \sum_{\lambda,\mathbf{k}} \sqrt{\frac{\hbar\omega_k}{2\epsilon_m V}} (e^{i\mathbf{k}\cdot\mathbf{r}} a_{\mathbf{k},\lambda} - e^{-i\mathbf{k}\cdot\mathbf{r}} a_{\mathbf{k},\lambda}^\dagger)\mathbf{e}_\lambda. \tag{G10}$$

We can now insert the shifted bosonic operator $\tilde{a}_{\mathbf{k},\lambda}$, defined in Eq. (G1), into this equation, which physically represents the fluctuations around the mean value $A_{\mathbf{k},\lambda}$. Therefore, the mean value of mode $\mathbf{k}$ of the displacement field is given by

$$\langle \mathbf{D}_{\mathbf{k}}\rangle = \epsilon_m \sum_{\lambda} \sqrt{\frac{\hbar\omega_k}{2\epsilon_m V}} (e^{i\mathbf{k}\cdot\mathbf{r}} + e^{-i\mathbf{k}\cdot\mathbf{r}}) A_{\mathbf{k},\lambda}\mathbf{e}_\lambda, \tag{G11}$$

where we considered that, by definition, $\langle \tilde{a}_{\mathbf{k},\lambda}\rangle = 0$. Using relation Eq. (G6), this mean value can be rewritten after some algebraic manipulations as

$$\langle \mathbf{D}_{\mathbf{k}}\rangle = \frac{d\sqrt{N}}{V} \sum_{\alpha} \sqrt{\frac{1}{2}\left(1 - \frac{1}{4\eta^2 f_{\mathbf{k}}^\perp}\right)} (e^{i\mathbf{k}\cdot\mathbf{r}} + e^{-i\mathbf{k}\cdot\mathbf{r}}) B_{\mathbf{k},\alpha}\mathbf{e}_\alpha, \tag{G12}$$

where $B_{\mathbf{k},\alpha}$ is defined by Eq. (G5).

Analogously, we can write the polarization field in terms of the bosonic operators as

$$\mathbf{P}(\mathbf{r}) = \frac{d\sqrt{N}}{V} \sum_{\alpha,\mathbf{k}} \left(e^{i\mathbf{k}\cdot\mathbf{r}} \sqrt{1 - \frac{1}{N}\sum_\beta b_{\mathbf{k},\beta}^\dagger b_{\mathbf{k},\beta}}\; b_{\mathbf{k},\alpha} + e^{-i\mathbf{k}\cdot\mathbf{r}} b_{\mathbf{k},\alpha} \sqrt{1 - \frac{1}{N}\sum_\beta b_{\mathbf{k},\beta}^\dagger b_{\mathbf{k},\beta}} \right) \mathbf{e}_\alpha. \tag{G13}$$

Using Eq. (G2) and taking the mean value of Eq. (G13), recalling that $\langle \tilde{b}_{\mathbf{k},\alpha}\rangle = 0$, we obtain the mean mode occupation of the transverse polarization field:

$$\begin{aligned} \langle \mathbf{P}_{\mathbf{k}}^\perp\rangle &= \frac{d\sqrt{N}}{V} \sum_\alpha (e^{i\mathbf{k}\cdot\mathbf{r}} + e^{-i\mathbf{k}\cdot\mathbf{r}}) B_{\mathbf{k},\alpha} \sqrt{1 - \frac{1}{N}\sum_\beta B_{\mathbf{k},\beta}}\; \mathbf{e}_\alpha \\ &= \frac{d\sqrt{N}}{V} \sum_\alpha \sqrt{\frac{1}{2}\left(1 - \frac{1}{4\eta^2 f_{\mathbf{k}}^\perp}\right)} (e^{i\mathbf{k}\cdot\mathbf{r}} + e^{-i\mathbf{k}\cdot\mathbf{r}}) B_{\mathbf{k},\alpha}\mathbf{e}_\alpha. \end{aligned} \tag{G14}$$

Thus, given the definition of the displacement field $\mathbf{D}(\mathbf{r}) = \epsilon_m \mathbf{E}^\perp(\mathbf{r}) + \mathbf{P}^\perp(\mathbf{r})$, the equality $\langle \mathbf{D}_{\mathbf{k}}\rangle = \langle \mathbf{P}_{\mathbf{k}}^\perp\rangle$ implies that the mean mode occupation of the electric field, $\langle \mathbf{E}_{\mathbf{k}}^\perp\rangle$, is zero. Moreover, we remark that the same mean field mode occupations are predicted even in the two-step Bogoliubov diagonalization, further confirming the ferroelectricity of the QPT. In fact, the mean occupation of the matter field is dictated only by the strength of dipolar interactions and not on the interaction with the radiation field.

As a final note, it is instructive to point out that if the factor $f_{\mathbf{k},\alpha,\beta}$ is regarded as a free parameter, we can recover from Hamiltonians (D10) and (G3) relevant known models and their behaviors near phase transitions. For instance, the Dicke model can be recovered by restricting the study only to the transverse modes and considering $f_{\mathbf{k},\alpha,\beta}^\perp = -\delta_{\alpha\beta}$ (implying $\tilde{f}_{\mathbf{k},\alpha,\beta}^\perp = 0$). As a consequence, relation (G8) reduces to the

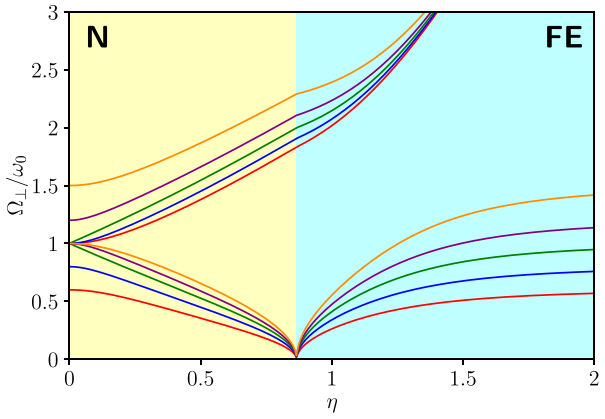

FIG. 5. Upper and lower polaritons as functions of η for different modes: $\omega_k/\omega_0 = 0.6$ (red), 0.8 (blue), 1 (green), 1.2 (purple), and 1.5 (yellow). The polaritons in the condensed ferroelectric phase are calculated by Eq. (G8).

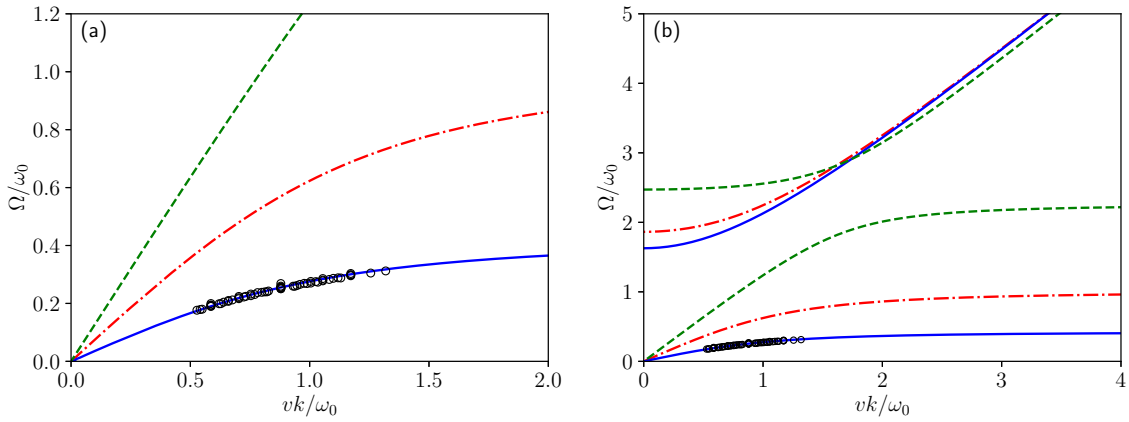

FIG. 6. Comparison between the theoretical models and experimental data in Ref. [39]: (a) region near the experimental data and (b) broader view including the upper polariton. As shown, the theoretical dispersion relation derived from the Hopfield-like model including the dipole-dipole interactions (solid blue) perfectly fits the experimental data (black dots). In contrast, the curves derived from the Dicke-like model (dashed green) and from the Hopfield model neglecting the dipolar interaction (red dash-dotted) significantly differ from the experimental data. The relevant parameters are $\eta' = 1.83$, $\omega_0 = 1.83$ eV, and $\epsilon_m = 1.96$, while the full set of parameters for the experimental curves is found in Ref. [39].

already known Dicke dispersion relation beyond the SPT [32]. Another notable case is $f^{\perp}_{\mathbf{k},\alpha,\beta} = 0$, corresponding to a pure Hopfield model, neglecting the dipole-dipole interactions. For such a model, the system of equations (G4) admits only the trivial solution, which is consistent with the well-known impossibility for a pure Hopfield Hamiltonian to undergo a phase transition.

APPENDIX H: CONNECTION TO EXPERIMENTAL DATA

In this final section, we further analyze and discuss the differences in the models, comparing them with the experimental data presented in Ref. [39], which refer to gold nanoparticle crystals with normalized light-matter coupling strength in the deep-strong coupling regime. Such a system falls under the model described in the main text, given the highly localized particles the polarization fields of which can be safely considered nonoverlapping. In Fig. 6, we present the comparison between the dispersion relations derived by a Dicke-like model, a Hopfield-like model including the dipole-dipole interactions, and a Hopfield-like model neglecting these interactions. These data are referred to a renormalized light-matter coupling $\eta' = 1.83$, corresponding to $\eta = 0.78$. The dispersion curves differ substantially for such high couplings: while the Hopfield model neglecting the dipolar interactions does not predict any QPT, the Hopfield-like model including this term is in the neighborhood of the ferroelectric QPT, whereas in the Dicke-like model the SPT has already taken place. Experimental measurements regarding the lower polariton are reported in the figure (black dots), which perfectly fits the theoretical predictions of the Hopfield-like model including the dipolar interactions, thus demonstrating its validity. On the other hand, these measurements are incompatible with the predictions of the other models. No data are available for the upper polariton given its high energy, which collocates it above the onset of the gold interband transitions.

[1] R. H. Dicke, Coherence in spontaneous radiation processes, Phys. Rev. **93**, 99 (1954).
[2] K. Hepp and E. H. Lieb, On the superradiant phase transition for molecules in a quantized radiation field: The dicke maser model, Ann. Phys. (NY) **76**, 360 (1973).
[3] W. R. Mallory, Solution of a multiatom radiation model using the Bargmann realization of the radiation field, Phys. Rev. **188**, 1976 (1969).
[4] Y. K. Wang and F. T. Hioe, Phase transition in the Dicke model of superradiance, Phys. Rev. A **7**, 831 (1973).
[5] F. T. Hioe, Phase transitions in some generalized Dicke models of superradiance, Phys. Rev. A **8**, 1440 (1973).
[6] K. Rzażewski, K. Wódkiewicz, and W. Żakowicz, Phase transitions, two-level atoms, and the A^2 term, Phys. Rev. Lett. **35**, 432 (1975).
[7] M. Yamanoi, Influence of omitting the A^2 term in the conventional photon-matter-Hamiltonian on the photon-field equation, Phys. Lett. A **58**, 437 (1976).
[8] M. Bamba and T. Ogawa, Stability of polarizable materials against superradiant phase transition, Phys. Rev. A **90**, 063825 (2014).
[9] T. Jaako, Z.-L. Xiang, J. J. Garcia-Ripoll, and P. Rabl, Ultrastrong-coupling phenomena beyond the Dicke model, Phys. Rev. A **94**, 033850 (2016).
[10] D. De Bernardis, T. Jaako, and P. Rabl, Cavity quantum electrodynamics in the nonperturbative regime, Phys. Rev. A **97**, 043820 (2018).
[11] D. De Bernardis, P. Pilar, T. Jaako, S. De Liberato, and P. Rabl, Breakdown of gauge invariance in ultrastrong-coupling cavity QED, Phys. Rev. A **98**, 053819 (2018).

[12] Y. Ashida, A. İmamoğlu, J. Faist, D. Jaksch, A. Cavalleri, and E. Demler, Quantum electrodynamic control of matter: Cavity-enhanced ferroelectric phase transition, Phys. Rev. X **10**, 041027 (2020).

[13] J. Keeling, Coulomb interactions, gauge invariance, and phase transitions of the Dicke model, J. Phys.: Condens. Matter **19**, 295213 (2007).

[14] J. M. Knight, Y. Aharonov, and G. T. C. Hsieh, Are superradiant phase transitions possible? Phys. Rev. A **17**, 1454 (1978).

[15] G. Mazza and A. Georges, Superradiant quantum materials, Phys. Rev. Lett. **122**, 017401 (2019).

[16] G. M. Andolina, F. M. D. Pellegrino, V. Giovannetti, A. H. MacDonald, and M. Polini, Cavity quantum electrodynamics of strongly correlated electron systems: A no-go theorem for photon condensation, Phys. Rev. B **100**, 121109(R) (2019).

[17] K. Lenk and M. Eckstein, Collective excitations of the $U(1)$-symmetric exciton insulator in a cavity, Phys. Rev. B **102**, 205129 (2020).

[18] G. M. Andolina, F. M. D. Pellegrino, A. Mercurio, O. Di Stefano, M. Polini, and S. Savasta, A non-perturbative no-go theorem for photon condensation in approximate models, Eur. Phys. J. Plus **137**, 1348 (2022).

[19] G. M. Andolina, F. M. D. Pellegrino, V. Giovannetti, A. H. MacDonald, and M. Polini, Theory of photon condensation in a spatially varying electromagnetic field, Phys. Rev. B **102**, 125137 (2020).

[20] J. Román-Roche, F. Luis, and D. Zueco, Photon condensation and enhanced magnetism in cavity QED, Phys. Rev. Lett. **127**, 167201 (2021).

[21] L. Garziano, A. Settineri, O. Di Stefano, S. Savasta, and F. Nori, Gauge invariance of the Dicke and Hopfield models, Phys. Rev. A **102**, 023718 (2020).

[22] C. Schäfer, M. Ruggenthaler, V. Rokaj, and A. Rubio, Relevance of the quadratic diamagnetic and self-polarization terms in cavity quantum electrodynamics, ACS Photonics **7**, 975 (2020).

[23] S. Hughes, C. Gustin, and F. Nori, Reconciling quantum and classical spectral theories of ultrastrong coupling: Role of cavity bath coupling and gauge corrections, Optica Quantum **2**, 133 (2024).

[24] D. Kim *et al.*, Observation of the magnonic Dicke superradiant phase transition, arXiv:2401.01873.

[25] A. Vukics, T. Grießer, and P. Domokos, Elimination of the A-square problem from cavity QED, Phys. Rev. Lett. **112**, 073601 (2014).

[26] A. Stokes and A. Nazir, Uniqueness of the phase transition in many-dipole cavity quantum electrodynamical systems, Phys. Rev. Lett. **125**, 143603 (2020).

[27] G. J. Daniels, R. D. Jenkins, D. S. Bradshaw, and D. L. Andrews, Resonance energy transfer: The unified theory revisited, J. Chem. Phys. **119**, 2264 (2003).

[28] G. A. Jones and D. S. Bradshaw, Resonance energy transfer: From fundamental theory to recent applications, Front. Phys. **7**, 100 (2019).

[29] A. Vukics and P. Domokos, Adequacy of the Dicke model in cavity QED: A counter-no-go statement, Phys. Rev. A **86**, 053807 (2012).

[30] A. Stokes and A. Nazir, Implications of gauge freedom for nonrelativistic quantum electrodynamics, Rev. Mod. Phys. **94**, 045003 (2022).

[31] J. J. Hopfield, Theory of the contribution of excitons to the complex dielectric constant of crystals, Phys. Rev. **112**, 1555 (1958).

[32] C. Emary and T. Brandes, Chaos and the quantum phase transition in the Dicke model, Phys. Rev. E **67**, 066203 (2003).

[33] C. Emary and T. Brandes, Quantum chaos triggered by precursors of a quantum phase transition: The Dicke model, Phys. Rev. Lett. **90**, 044101 (2003).

[34] M. H. Cohen and F. Keffer, Dipolar sums in the primitive cubic lattices, Phys. Rev. **99**, 1128 (1955).

[35] N. N. Bogoljubov, On a new method in the theory of superconductivity, Nuovo Cimento **7**, 794 (1958).

[36] O. Di Stefano, A. Settineri, V. Macrì, L. Garziano, R. Stassi, S. Savasta, and F. Nori, Resolution of gauge ambiguities in ultrastrong-coupling cavity QED, Nat. Phys. **15**, 803 (2019).

[37] S. Savasta, O. Di Stefano, A. Settineri, D. Zueco, S. Hughes, and F. Nori, Gauge principle and gauge invariance in two-level systems, Phys. Rev. A **103**, 053703 (2021).

[38] C. Gustin, S. Franke, and S. Hughes, Gauge-invariant theory of truncated quantum light-matter interactions in arbitrary media, Phys. Rev. A **107**, 013722 (2023).

[39] N. S. Mueller, Y. Okamura, B. G. M. Vieira, S. Juergensen, H. Lange, E. B. Barros, F. Schulz, and S. Reich, Deep strong light-matter coupling in plasmonic nanoparticle crystals, Nature (London) **583**, 780 (2020).

[40] P. Nataf and C. Ciuti, No-go theorem for superradiant quantum phase transitions in cavity QED and counter-example in circuit QED, Nat. Commun. **1**, 72 (2010).

[41] M. O. Scully and M. S. Zubairy, *Quantum Optics* (Cambridge University, Cambridge, England, 1997).

[42] M. Yamanoi and M. Takatsuji, *Coherence and Quantum Optics IV: Proceedings of the Fourth Rochester Conference on Coherence and Quantum Optics* (Plenum, New York, 1978).

[43] S. Lamowski, C.-R. Mann, F. Hellbach, E. Mariani, G. Weick, and F. Pauly, Plasmon polaritons in cubic lattices of spherical metallic nanoparticles, Phys. Rev. B **97**, 125409 (2018).

[44] S. Savasta and R. Girlanda, Quantum description of the input and output electromagnetic fields in a polarizable confined system, Phys. Rev. A **53**, 2716 (1996).

[45] A. Frisk Kockum, A. Miranowicz, S. De Liberato, S. Savasta, and F. Nori, Ultrastrong coupling between light and matter, Nat. Rev. Phys. **1**, 19 (2019).

[46] A. Vukics, T. Grießer, and P. Domokos, Fundamental limitation of ultrastrong coupling between light and atoms, Phys. Rev. A **92**, 043835 (2015).

[47] T. Grießer, A. Vukics, and P. Domokos, Depolarization shift of the superradiant phase transition, Phys. Rev. A **94**, 033815 (2016).

[48] D. Lamberto, G. Orlando, and S. Savasta, Superradiant quantum phase transition in open systems: System-bath interaction at the critical point, arXiv:2411.16514.

[49] C. Cohen-Tannoudji, J. Dupont-Roc, and G. Grynberg, *Photons and Atoms: Introduction to Quantum Electrodynamics* (Wiley, New York, 1989).